

## Understanding the retinal basis of vision across species

Article (Published Version)

Baden, Tom, Euler, Thomas and Berens, Philipp (2020) Understanding the retinal basis of vision across species. *Nature Reviews Neuroscience*, 21 (1). pp. 5-20. ISSN 1471-003X

This version is available from Sussex Research Online: <http://sro.sussex.ac.uk/id/eprint/89378/>

This document is made available in accordance with publisher policies and may differ from the published version or from the version of record. If you wish to cite this item you are advised to consult the publisher's version. Please see the URL above for details on accessing the published version.

### **Copyright and reuse:**

Sussex Research Online is a digital repository of the research output of the University.

Copyright and all moral rights to the version of the paper presented here belong to the individual author(s) and/or other copyright owners. To the extent reasonable and practicable, the material made available in SRO has been checked for eligibility before being made available.

Copies of full text items generally can be reproduced, displayed or performed and given to third parties in any format or medium for personal research or study, educational, or not-for-profit purposes without prior permission or charge, provided that the authors, title and full bibliographic details are credited, a hyperlink and/or URL is given for the original metadata page and the content is not changed in any way.

## Understanding the retinal basis of vision across species

Tom Baden<sup>1,2\*</sup>, Thomas Euler<sup>2,3</sup> and Philipp Berens<sup>2,3,4,5</sup>

**Abstract** | The vertebrate retina first evolved some 500 million years ago in ancestral marine chordates. Since then, the eyes of different species have been tuned to best support their unique visuoeological lifestyles. Visual specializations in eye designs, large-scale inhomogeneities across the retinal surface and local circuit motifs mean that all species' retinas are unique. Computational theories, such as the efficient coding hypothesis, have come a long way towards an explanation of the basic features of retinal organization and function; however, they cannot explain the full extent of retinal diversity within and across species. To build a truly general understanding of vertebrate vision and the retina's computational purpose, it is therefore important to more quantitatively relate different species' retinal functions to their specific natural environments and behavioural requirements. Ultimately, the goal of such efforts should be to build up to a more general theory of vision.

### Visual field

The area in space that an animal can simultaneously survey using its eyes.

### Efficient coding hypothesis

A theory that posits that the retina has evolved to encode the visual environment efficiently: that is, by minimizing the redundancy in the information carried by different neurons.

Animals use vision to navigate their vastly different environments, whether they are deep-water marine species communicating with bioluminescent displays or birds scanning their environment for prey from high up in the air. The eyes of each animal are exquisitely adapted to allow it to gather the information from its environment that is needed for its survival and procreation<sup>1,2</sup>. Many adaptations to the visual properties of specific environments are evident in the structure and function of the retinal circuits of particular species (for example, the ratio of rod to cone photoreceptors often depends on the time of day that an animal is most active)<sup>1–6</sup>. However, the comparative studies that are necessary to understand more generally how such adaptations relate to the ecological context of different species and to ultimately arrive at a truly general theory of vision will require detailed knowledge of retinal circuit structure and function across species. Such knowledge may also have a broader impact: it is likely that studies of other neural circuits will profit from a deep understanding of the circuits, computational strategies and coding principles that operate in the retina.

Recent studies have started to reveal the extent to which the retinas of some species are adapted to the statistics of the visual information that they receive, such as the distribution of spatial, temporal and spectral information, as well as to their specific behavioural demands<sup>3,6–12</sup>. These studies have demonstrated that retinal circuits may differ even between closely related species<sup>1,2</sup>. Furthermore, even within a single species, visual input statistics and behavioural demands can be very different across the visual field, and studies have shown

that retinal circuits also strongly vary across the retinal surface<sup>1,2,10,11</sup>. These considerations have sparked a new wave of studies probing retinal circuit organization in the context of its function, assessed using natural rather than artificial inputs<sup>4,13,14</sup>.

Here, we review the latest developments in this field, with an emphasis on the discovery of species differences and functional distinctions across the retina. We consider what these findings mean for long-held theoretical notions that the retina is adapted to encode the environment of a species efficiently (the so-called efficient coding hypothesis)<sup>15,16</sup>. Finally, we show how current technological developments are starting to provide us with important insights into the ways in which retinal function is constantly retuned to meet ever-changing visual demands.

### Retinal organization and diversity

**Retinal cell types and their function.** The vertebrate retina comprises five classes of neurons that are arranged into three nuclear and two synaptic layers<sup>17,18</sup> (FIG. 1). In the first synaptic layer, the outer plexiform layer, photoreceptors (comprising rods and cones) release glutamate onto the dendrites of bipolar cells and horizontal cells. Horizontal cells connect laterally to provide feedback and feedforward signals to both photoreceptors and bipolar cells (reviewed in REFS<sup>19,20</sup>). Bipolar cells in turn project to the second synaptic layer in the inner retina, the inner plexiform layer. There they contact dendritic processes of amacrine cells and retinal ganglion cells (RGCs) (reviewed in REF<sup>21</sup>). Like horizontal cells, amacrine cells connect laterally but they also connect across

<sup>1</sup>Sussex Neuroscience, School of Life Sciences, University of Sussex, Brighton, UK.

<sup>2</sup>Institute for Ophthalmic Research, University of Tübingen, Tübingen, Germany.

<sup>3</sup>Werner Reichardt Centre for Integrative Neuroscience, University of Tübingen, Tübingen, Germany.

<sup>4</sup>Institute for Bioinformatics and Medical Informatics, University of Tübingen, Tübingen, Germany.

<sup>5</sup>Bernstein Centre for Computational Neuroscience, University of Tübingen, Tübingen, Germany.

\*e-mail: [t.baden@sussex.ac.uk](mailto:t.baden@sussex.ac.uk)

<https://doi.org/10.1038/s41583-019-0242-1>

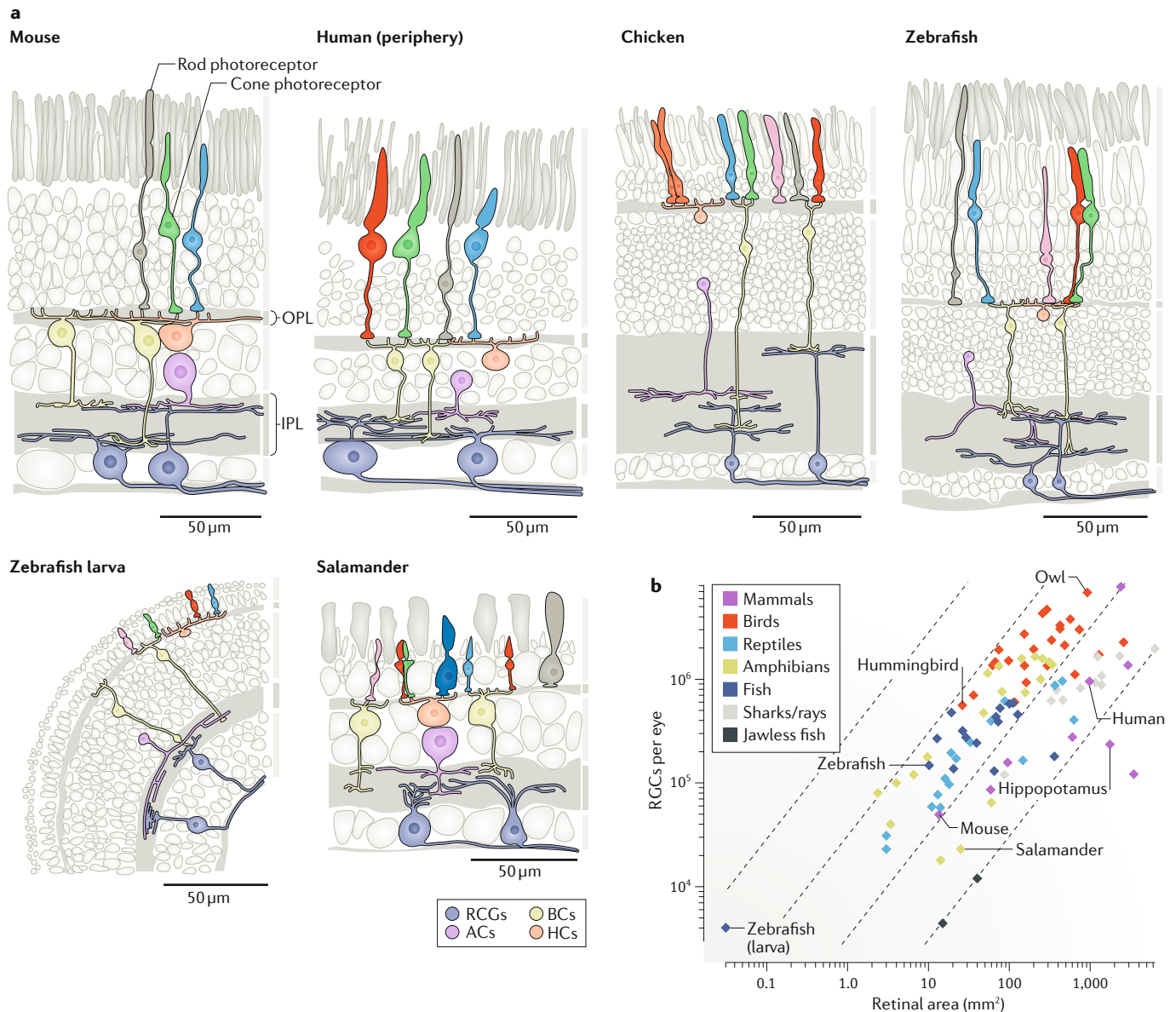


**Fig. 1 | Retinal composition across species.** **a** | The cell types present in the retinas of several contemporary vertebrate species (shown as transverse sections). For comparison, the plexiform (synaptic) layers (the outer plexiform layer (OPL) and inner plexiform layer (IPL)) are demarcated alongside each image. Example morphologies of different retinal neuron classes are highlighted. The schematics were created on the basis of data from the following references: mouse<sup>191</sup>, human<sup>192</sup>, chicken<sup>193</sup>, zebrafish adult<sup>194</sup>, zebrafish larva<sup>195</sup> and salamander<sup>196</sup>. **b** | Graph showing the total number of retinal ganglion cells (RGCs) present in the retinas of 105 different species versus their retinal surface area. For comparison, isodensity lines (indicating constant densities) are shown as dashed lines.

The graph was created using data from REFS<sup>3,71,85–87,89,92,104,108,124,126,173,197–234</sup>. Species were selected for inclusion on the basis of the availability of quantitative RGC information for those species in the literature. For each clade for which such information was available, we selected one to four articles for inclusion on the basis of how readily the data could be extracted from a given study. Naturally, this list is therefore non-exhaustive. Detailed information is available in Supplementary Table 1. It can be seen that (in general) larger eyes comprise proportionally more RGCs. However, for any given eye size, RGC numbers across species vary by more than two orders of magnitude. Colours are used to distinguish between major clades of the vertebrate lineage. AC, amacrine cell; BC, bipolar cell; HC, horizontal cell.

#### Centre-surround receptive fields

An area in visual space or on the retinal surface where presentation of a stimulus in the receptive field centre excites the neuron and presentation of the same stimulus in the receptive field surround (a typically larger and concentric area) instead suppresses the neuron.

the inner plexiform layer to provide mostly inhibitory feedback and feedforward signals (reviewed in REFS<sup>22–25</sup>). Finally, RGCs integrate synaptic inputs across their dendrites and send this information to the brain via the optic nerve (reviewed in REFS<sup>26,27</sup>).

**The mouse retina as a benchmark.** The fundamental retina blueprint outlined in the previous section is highly conserved across species, as are several aspects of its

general functional organization. For example, neurons present at different circuit levels within vertebrate retinas consistently use centre-surround receptive fields<sup>28</sup> and rely heavily — though not exclusively<sup>29–35</sup> — on analogue processing of visual information, before its arrival at the dendrites of RGCs (reviewed in REF.<sup>36</sup>). Nonetheless, there are only a few species for which we have a detailed understanding of the anatomical and functional properties of individual retinal circuits, the most notable of

### Clades

Groups of species that share a phylogenetic branch.

### Midget pathway

A circuit motif found in the primate retina consisting of cone photoreceptors, midget bipolar cells and midget retinal ganglion cells. A distinguishing feature of the midget pathway is that it exhibits a 1:1:1 connectivity from cones to retinal ganglion cells at the foveal centre.

which is the mouse (reviewed in REF.<sup>37</sup>). In addition to detailed studies on specific circuits, such as the pathway that feeds rod photoreceptor signals into cone photoreceptor circuits<sup>38</sup> or the circuits that compute the direction of motion<sup>39</sup>, a near-complete parts list (that is, an account of all of the neuron types that make up a given class of neuron) is available for most retinal cell classes in the mouse<sup>37,40–47</sup>. From these studies we know that, in the mouse retina, the signals of three photoreceptor types and one horizontal cell type are distributed to a set of 14 bipolar cell types, modulated by some 40 amacrine cell types and relayed to the brain via 40–50 types of RGCs.

This rich knowledge of the mouse retina's neuronal building blocks has allowed targeted studies into circuit mechanisms that offer a key to understanding the underlying computational principles of the retina and — perhaps — insights into the functional purpose of the retina. For example, we now know that in the mouse retina there are at least eight types of direction-selective RGC<sup>48,49</sup>, at least four types of orientation-selective RGC<sup>49–53</sup>, two pairs of 'alpha' RGCs (characterized by their large receptive fields)<sup>49,54</sup>, four 'ultra-small-field' RGCs<sup>49,55,56</sup>, a wealth of RGCs that encode visual features such as image blur<sup>57</sup>, looming<sup>58</sup> and uniformity<sup>49,59</sup> (often referred to as being suppressed by contrast)<sup>60</sup> and several intrinsically photosensitive RGCs<sup>61</sup>. Similarly detailed functional characterizations of key amacrine cells are available: these include the AII and A17 amacrine cells, which shape rod pathway signalling<sup>62,63</sup>, and the more recently described VGLUT3-expressing amacrine cells, which act as a central hub for motion-sensitive RGC circuits<sup>64–67</sup>. While our knowledge of most amacrine cell types is still incomplete<sup>22,37</sup>, the aforementioned examples reveal circuit motifs that underpin a wide range of retinal functions. Thus, the findings of anatomical, functional, computational and genetic studies in mice are beginning to converge into the first coherent picture of a mammalian retina.

What does this accumulated knowledge tell us about the fundamental principles that govern animal vision? After all, the mouse is but one species, with its own set of species-specific needs, behavioural repertoires and evolutionary history. If we ever were to truly understand this specific retina (and despite the rosy picture painted above, we are still a long way from such an understanding), what might this teach us about vision in other species, including our own? To gain insight into the general principles of retinal function<sup>68</sup>, it will be critical to build a better understanding of which aspects of the mouse retina reflect general circuit principles and which are particular to mice, mammals or species with a similar visuoecological niche. For this, we need to study the retinas of at least a handful of other species at similar depth.

**Structural and functional retinal diversity.** The retinas of all sighted vertebrates on Earth today stem from an ancient circuit blueprint that first evolved in early marine vertebrates more than 500 million years ago (BOX 1). Since then, the retinas of different species have therefore had up to 500 million years to adjust their structure and function to species' needs. Indeed, starting with the work of Ramon y Cajal<sup>69</sup> and contemporaries, a more

than 120-year history of comparative anatomy reveals a sizable diversity of retinal layouts across contemporary vertebrate eyes (FIG. 1a). Some retinas — such as those of salamanders — appear structurally simple, with small numbers of large cell bodies flanking relatively thin synaptic layers<sup>70</sup>. Other retinas appear to be rather complex, such as those of birds, with thick synaptic plexi and stacks of cell bodies in every nuclear layer<sup>71–73</sup>. This diversity prompts us to ask what each animal's eyes tell its brain<sup>74</sup>: do all retinas transmit the same amount and kind of information to the brain or does the apparent 'complexity' of a species' retina reflect the type and complexity of the information that it transmits? Here, retinal complexity is defined by features that include the density and interconnectedness of its neural processes, while 'computational complexity' refers to the extent to which visual information is preprocessed before it leaves the retina, as well as its functional diversity.

The amount of information that can be passed from the retina to the brain per unit of retinal surface area might be assumed to approximately scale with RGC density, which has been measured for hundreds of vertebrates<sup>75</sup> (Supplementary Table 1). A preliminary overview of the information on RGC density that is currently available in the literature (FIG. 1b) raises the notion that animals belonging to different clades tend to exhibit different approximate RGC densities. For example in our limited sample, most birds and reptiles appear to feature higher RGC densities than most mammals or sharks<sup>75</sup>. It is also clear that animals with vastly different eye sizes can have similar overall numbers of RGCs. For example, the human retina has a surface area that is 30 times that of the hummingbird retina<sup>71</sup> but possesses only three times as many RGCs<sup>76</sup>. On the other hand, the sizes of mouse and hummingbird eyes are similar, yet mice have almost an order of magnitude fewer RGCs<sup>77</sup>.

Does the increased RGC density of the retinas of certain species (such as the hummingbird) make them more computationally complex than the retinas of other species (such as mice and humans) and thus able to transmit more information to the brain? The answer is that we do not yet know: a high RGC density could indeed be a consequence of higher computational complexity as it could allow more parallel feature processing channels; however, it may simply relate to a higher spatial acuity as a result of a higher RGC density per processing channel. These two factors are fundamentally entwined in any given retina, meaning that examining RGC densities alone is unlikely to yield a satisfactory answer. Instead, it will be vital to develop a deeper understanding of the functional, structural and genetic diversity of different animals' retinal outputs.

### What drives retinal diversity?

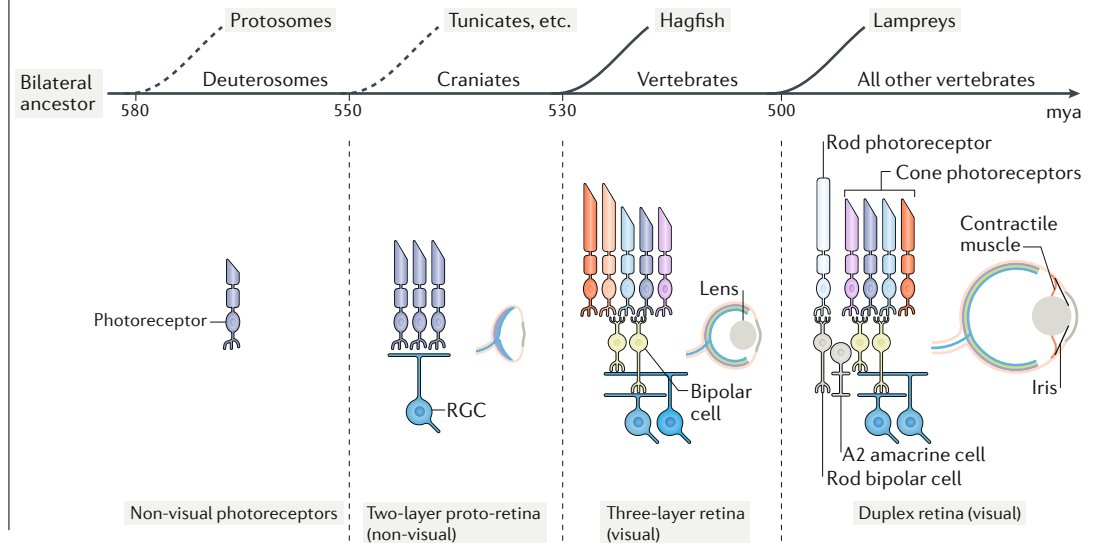
It has been posited that the dumber the animal, the smarter the retina<sup>78,79</sup>. In support of this idea, primate vision heavily relies on the midget pathway, perhaps one of the simplest of all retinal circuits. In this pathway, which is numerically dominant across the primate retina<sup>80</sup>, signals generated by photoreceptors are more or less directly relayed via bipolar cells to RGCs and there are few inner retinal inhibitory connections (a hallmark



Box 1 | The evolution of the vertebrate retina

At the end of the Cambrian explosion, the three-layered duplex retina common to all classes of jawed vertebrates — which include cartilaginous and bony fish, amphibians, reptiles, birds and mammals — evolved over a period of less than 100 million years<sup>171,172</sup> (see the figure showing the approximate timeline of vertebrate retinal evolution, based on data reviewed in REF.<sup>173</sup>). What initially was likely to have been a mere collection of non-image-forming, ciliated photoreceptors evolved into a simple, two-layer proto-retina about 550 million years ago (mya), as can still be seen today in a ‘living fossil’, the hagfish<sup>171,173</sup>. These earliest jawless vertebrates (of the class Myxini) diverged from the jawed vertebrate lineage 530 mya and their lensless eyes, which are buried beneath a transparent layer of skin, mostly serve circadian functions and for basic light detection<sup>171</sup>. Around the same time, fossil records show that two other groups of early stem-vertebrates, those of the genera *Metaspriggina*<sup>174</sup> and *Haikouichthys*<sup>175,176</sup>, emerged: like hagfish, these soft-bodied fish had camera-type eyes (that is, eyes that use a single lens, presumably to focus light onto a retina lining the back of the eyeball) but, at least macroscopically, their eyes were already remarkably reminiscent of those of small contemporary teleosts such as zebrafish<sup>174</sup>.

Did these animals feature the earliest image-forming retinas in vertebrates? Here, another group of living fossils, the lampreys (Cephalaspidomorphi), provide important insights. Lampreys diverged from our lineage ~30 million years after hagfish and were equipped with both camera-type eyes with a lens and, importantly, interneurons (bipolar cells)<sup>171</sup> that connected a diverse set of ciliated photoreceptors to the retina’s output neurons, the retinal ganglion cells (RGCs)<sup>173,177</sup>. This suggests that the three-layered retina evolved between 530 and 500 mya and may thus have been present in stem vertebrates such as members of the genera *Metaspriggina* and *Haikouichthys*. This early retina still may have lacked rod photoreceptors and their postsynaptic circuits<sup>171,178</sup>; however, it is likely that such rod pathways emerged shortly after<sup>171</sup>. In parallel, the contractile iris and muscles attached to the lens to allow for accommodation evolved, as seen in modern-day sharks, rays and skates (of the class Chondrichthyes), which diverged from our lineage at least ~420 mya (REFS<sup>179,180</sup>). Taken together, these findings show that the major features of the vertebrate retina are truly ancient.



of more complex retinal circuits<sup>81</sup>. Rodents, on the other hand, lack an obvious midget pathway and instead feature a more balanced mix of different types of retinal circuits<sup>49</sup>. Finally, zebrafish feature a retina with an RGC density that rivals that of birds<sup>82,83</sup>, and in which bipolar cells exhibit a number of complex functional properties that have traditionally been associated with RGCs in mammalian retinas (discussed later). Because half of all the central neurons of larval zebrafish are located in their eyes<sup>3</sup>, their visual processing is heavily ‘front-loaded’ and it can be hypothesized that this necessitates a more sophisticated output from the eye in this species than in other species. Indeed, a similar concept was famously put forward in Lettvin’s ‘bug detector’ neurons of the frog retina<sup>74</sup>. In further support of this idea, a recent computational study that used deep neural networks with a bottleneck architecture to model visual pathways showed that, in order to maintain coding accuracy, a more ‘complex’ retina is required to compensate for a ‘simpler’ brain (that is, one with fewer non-linear processing layers)<sup>84</sup>.

However, the proposed inverse relationship between retinal circuit complexity and brain processing capacity breaks down when vertebrates are considered more broadly. For example, the RGC densities of birds<sup>71,85</sup> and some frogs<sup>86</sup> appear to be similar, as do those of mammals and sharks<sup>87</sup> — despite the presumably more ‘complex’ brains of birds and mammals compared with those of frogs and sharks. Clearly, the computational power of an animal’s central brain (alone) does not predict retinal complexity. Instead, we might expect other factors to dominate. These include eye size, photoreceptor complement and, perhaps most importantly, species-specific visual needs.

**Eye and animal size.** As eyes become larger, physical constraints on vision change. Both spatial resolution and the absolute number of photons available for vision increase due to improved optics. Larger eyes project a larger image at the level of photoreceptor outer segments, but retinal neurons do not necessarily become

**Deep neural networks**  
Machine learning algorithms consisting of many processing layers that combine linear operations such as convolutions with non-linear stages such as rectification. Such networks have been shown to achieve human-like performance in many visual tasks.

**Visual angle**

The angle that encompasses a certain feature in the visual world, from the point of view of an animal's eye.

**Colour-opponent RGCs**

Retinal ganglion cells (RGCs) that are excited by the presentation of light at one range of wavelengths and suppressed by presentation of light at another range of wavelengths.

**Binocular region**

The region in the visual space that is simultaneously surveyed by both eyes.

**Goal-directed saccades**

Rapid eye movements that bring specific objects into a retinal region's field of view.

larger<sup>88,89</sup>. Therefore, as eye size increases, more neurons can be packed into the retina per visual angle, which might result in increased spatial resolution or make room for new retinal circuits (and thus could increase retinal complexity). On the other hand, increased eye size also allows circuits to be spread out to keep retinal thickness in check (this is critical as light and oxygen must penetrate the retinal layers to reach the photoreceptors<sup>90</sup>), which might be hypothesized to reduce retinal complexity. Furthermore, once the eye reaches a certain size, other factors appear to influence the organization of retinal circuits. For example, in the primate eye spatial resolution is sacrificed in the peripheral retina despite perfectly good optics. It has been suggested that this keeps the size of the optic nerve manageable at about one million axons per eye<sup>91</sup>; however, it can be argued that bandwidth on the optic nerve alone cannot explain this arrangement. The Chilean eagle, for example, has approximately ten million RGCs per eye<sup>85</sup>, nearly ten times more than humans despite similar-sized eyes.

As eye size increases, absolute distances on the retinal surface per degree of visual angle increase. Therefore, any computations that require the retina to integrate information over large receptive fields must adapt. For example, mice and rabbits have very different eye sizes, meaning that the image of an object moving the same distance in the outside world traverses very different absolute distances on each of their retinas' surfaces. As a result, the two species cannot use the exact same neural implementation for motion computation: indeed, recent work has shown that the need to match motion velocity to eye size has driven distinct dendritic wiring motifs in the motion detection circuits of these two animals<sup>88</sup>. Thus, factors such as eye size can constrain how a specific computation can be implemented and this, in turn, might lead to the need to organize circuits differently in different species.

Taking the eye size-related constraints on implementation to the extreme, in the 300- $\mu$ m-diameter eye of larval zebrafish, RGC dendrites span some 10° of visual space in a mere 30  $\mu$ m (REF.<sup>92</sup>). Therefore, the retina of this animal can compute across large parts of visual space using small and presumably electrotonically compact neurons. At least some intraretinal strategies for feature computation in these small fish's eyes differ from those in mammals. For example, mouse and rabbit retinal circuits feature several types of orientation-selective RGCs, which become orientation selective due to the interaction of non-orientation-selective bipolar cell input with input from amacrine cells at the RGC level<sup>50–52</sup>. In contrast, recent work suggests that larval zebrafish already exhibit orientation selectivity at the level of their bipolar cells<sup>93,94</sup>. To what extent this organizational principle persists in the larger adults remains to be tested. Different computational strategies in animals such as larval zebrafish may also be necessitated by their tiny RGC axon diameters (often less than 100 nm (REF.<sup>95</sup>), compared with 300–2,500 nm in humans<sup>76</sup>), which it can be hypothesized could make them unreliable in propagating action potentials<sup>96,97</sup>, and hence may require larval zebrafish RGCs to use a different 'code' to talk to the brain. However, these ideas still require experimental exploration.

**Photoreceptor complement.** Retinal circuit differences may also be linked to an animal's photoreceptor complement. The vertebrate standard — which applies to many fish, amphibians, reptiles and birds — uses up to five spectral cone photoreceptor types and one or two rod photoreceptor types<sup>98,99</sup>. In contrast, most mammals possess only two types of cone and one type of rod, while most marine mammals and sharks have even fewer photoreceptor types<sup>100,101</sup>. The reduced photoreceptor complement might be hypothesized to drive reduced retinal complexity in these species because fewer circuits for comparing chromatic channels are required<sup>21,45,83</sup>. In support of this idea, the retina of freshwater turtles, which is known to perform rich colour computations, contains more than ten distinct varieties of colour-opponent RGCs<sup>102</sup>, compared with the typical mammalian two or three<sup>103</sup>. However, there are numerous exceptions to this rule: for example, salamanders and frogs have similar photoreceptor complements<sup>98,99</sup>, but the retina of frogs tends to be much more complex than that of salamanders<sup>74,104</sup>. Notably, it has been shown that strong correlations in the spectral structure of natural light mean that the theoretical information benefit of increasing photoreceptor diversity and the number of different colour-opponent circuits rapidly declines as their number increases<sup>105,106</sup>. Accordingly, adding ever-more spectral photoreceptor types and associated colour-opponent retinal circuits is unlikely to substantially increase the amount of spectral information that can be harnessed from most natural scenes. On the other hand, some groups of animals (such as many birds)<sup>107</sup> produce complex reflectance patterns on their body surfaces, which may be linked to the existence of diverse spectral photoreceptor types, and it may therefore be the case that these species stand to disproportionately gain from the use of multiple spectral detectors for social signalling.

**Viewing strategy and visual requirements.** Depending on an animal's visuoecological needs — for example, avoiding predators as prey or being a predator itself — its eyes can be positioned either to the sides of the head, yielding horizontal viewing angles of up to 170° per eye (in rabbits)<sup>108</sup>, or in the front of the head, allowing a large binocular region and improved depth estimation (as in case of cats)<sup>109</sup>. Eye position also affects viewing strategy. For example, while rodents do make goal-directed saccades<sup>110</sup>, an important role of their eye movements is to stabilize the retinal image in the presence of head and body motion, while simultaneously using their extended visual field to survey their environment for the presence of potential threats<sup>110,111</sup>. In contrast, many primates, including humans, reconstruct their visual world by scanning their environment. This viewing strategy is likely a consequence of having a fovea — a small central retinal region in which cone density is maximal and the neural circuits are tailored for high-acuity vision (such that some complex computations are shifted downstream, as discussed earlier) and even laterally displaced on the retinal surface to improve optical properties. Hence, in primates, the combination of a foveated, spatially limited field of view with highly motile eyes ensures good spatial acuity while gathering substantial

## Box 2 | Five additional factors that drive eye design

### Energy

Neurons are some of the most energy-demanding cells of the body, and photoreceptors (and to some extent, bipolar cells) are particularly energetically expensive (reviewed in REF.<sup>181</sup>). They are constantly partially depolarized, release large numbers of synaptic vesicles, use extensive secondary messenger cascades and rapidly shed outer-segment discs. Perhaps as a consequence of this energy demand, malfunction in vision is often associated with damage to photoreceptors rather than to damage to the downstream visual network (reviewed in REF.<sup>182</sup>). Indeed, the rapid evolutionary speed at which cave-fish eyes atrophied following constant-dark enclosure<sup>183,184</sup> suggests that the energy required for eye function is limiting for any species. We might expect small species with relatively large eyes to be affected most strongly. Some animals switch off their retina during periods of disuse: for example, ground squirrels disassemble their photoreceptor synaptic machinery during hibernation<sup>185</sup> and zebrafish do the same every night<sup>186</sup>. In other species, a compromise might be to reduce the baseline activity of photoreceptors to save energy (as in the case of cones in the ventral part of the mouse retina)<sup>6</sup>. Thus, one might expect to find different coding strategies (and different retinal designs) in different species as a direct consequence of the strategies to reduce energy expenditure that they have evolved.

### Body temperature

Like all biological processes, the speed of neuronal functions depends on temperature. Accordingly, an eye's computational repertoire will be affected by an animal's body temperature, which can vary strongly over the course of the day or season. To date, the effects of temperature variations on retinal design and function remain scarcely explored, yet it is clear that some basic properties, such as the amplitudes of neuronal responses in the retina to a flash of light, can be markedly attenuated after cooling<sup>187</sup>.

### Diurnal versus nocturnal lifestyle

The absolute amount of available light, its wavelength distribution and the types of visual features that are behaviourally important all depend on the time of day and will thus have an impact on eye design. Examples of such an impact can be seen in the increased eye sizes of primates that are predominantly nocturnal versus those that are diurnal<sup>188</sup> and in the link between the presence of behaviourally relevant information in the UV band<sup>189</sup> and the UV sensitivity of some birds<sup>168</sup>.

### Visual clutter

Depending on an animal's natural habitat and behavioural patterns, their probability of encountering different types of visual features will differ. For example, in the open ocean there is typically little background clutter, which facilitates spotting objects in the foreground, while the shallows offer a much more cluttered visual environment. Such differences seem to be reflected in the distribution of retinal ganglion cells (RGCs) in different species (FIG. 2e): for example, the horizontally elongated RGC density in the retinas of red kangaroos may be an adaptation to these animals inhabiting plains with little visual clutter. By contrast, the local RGC density seen in tree kangaroos appears to be better for visual parsing of a highly cluttered forest habitat<sup>120</sup>.

### Visual interaction range

While eagles must spot prey hundreds of metres beneath them, what happens but a few centimetres away is likely of little consequence to larval zebrafish. The range of distances over which animals typically observe the world impacts many aspects of an animal's visual experience, including the temporal, spatial and spectral statistics of visual features that can be detected. For example, when underwater, spectral filtering<sup>190</sup> means that objects become increasingly monochromatic at distance.

near-peripheral visual information to guide attention and future focusing. Yet, to see things behind them, humans must turn their head. Foveated birds seem to pursue a viewing strategy similar to that of primates: although, unlike primates, their eyes often have low motility, they make up for this with exploratory head movements<sup>112</sup>, and these movements are more readily deployed in species in which a larger proportion of the retina is taken up by a fovea<sup>112</sup>. This is not so for the chameleon or the sandlance (a small fish): their telescope-like eyes allow only a tiny field of view, but their protruding eyeballs can independently rotate to allow them to effectively look forward and backward at the same time<sup>113</sup>.

In addition to the eye motility discussed above, a feature of vertebrate vision is the presence of small and fast angular displacements of the eye's optical axis (fixational eye movements). In general, the average size of these fixational eye movements<sup>114</sup> can be related to the average receptive field diameters in a species' retina and the size of its visual field<sup>115</sup>, suggesting that these eye movements contribute to providing the visual system with uncorrelated inputs in natural scenes.

How these considerations link to variations in the functional properties of the retinal circuits of these species remains to be established. However, a comparison of a well-studied circuit, the retinal direction-selective circuit, across species may provide some insight. Mice, rabbits, salamanders and turtles all feature a rather conserved set of direction-selective RGCs; however, primates seem to lack a similarly rich complement of direction-selective cells (reviewed in REF.<sup>48</sup>; but see REF.<sup>116</sup>) and instead seem to compute the direction of motion in the cortex (reviewed in REF.<sup>48</sup>). It can be hypothesized that the dominance of active exploratory eye movements in primates, in combination with the need to send signals from single cone photoreceptors to the brain to maximize spatial acuity at the foveal centre, means that the computation of motion direction in the eye is secondary to other requirements. However, how differences in vertebrates' viewing strategies, eye movements and lifestyles can be linked to functional differences at the level of their retinal circuits remains scarcely explored outside primates. To answer this question, it will therefore be important to systematically gather large-scale physiological datasets from a range of species under different experimental conditions, and to link these with their respective natural statistics and behavioural demands.

Finally, other major factors that drive retinal design include energy limitations, body temperature, lifestyle, the statistics of the scenes that are viewed (such as a habitat's visual clutter) and an animal's behavioural and visual interaction range (BOX 2). Together, these factors mean that the likelihood of encountering specific visual features in different animals' natural visual worlds, their usefulness for guiding important behavioural decisions and the ability of the nervous system to detect and process these features all are highly species specific. We should therefore expect the organization of retinal circuits and their computations to reflect this species specificity.

### Regional retinal specializations

The visual world is highly diverse. This is the case not only when we are comparing the natural environments inhabited by different species, but also when we compare the different parts of the visual field of a single species. Most prominently, many sighted animals live in a visual world that is segregated along the vertical axis. For land-living animals, the horizon often bisects the world into the ground, where food and mates are likely to be found, and an upper visual field covering the sky, a region where aerial predators might appear<sup>6,117</sup> (FIG. 2a,b). High up in the sky, birds experience a similarly bisected world (FIG. 2c), and in addition may encounter different navigational information in the sky and on

the ground. For animals that live beneath the water surface, the vertical axis can carry multiple instances of stepwise variations in brightness, spectrum and visual clutter<sup>3</sup> (FIG. 2d). For example, in the shallow freshwaters inhabited by zebrafish, the ground is near and offers the greatest spatial detail. The horizon looks along the water column and tends to be featureless, except for objects in the foreground. Immediately above the horizon is a scattered reflection of the ground, and, finally, Snell's window<sup>118</sup> (the region directly above the animal) contains a

typically featureless view of mostly sky above the water. Presumably as a direct consequence of the fact that properties of the visual input change across scenes, the neural circuits processing different parts of the visual field within the same species have often evolved to perform different sets of computations.

**Regional variability in RGC density.** These adaptations start in the retina, as is immediately apparent when one is looking at the much-studied density distributions of

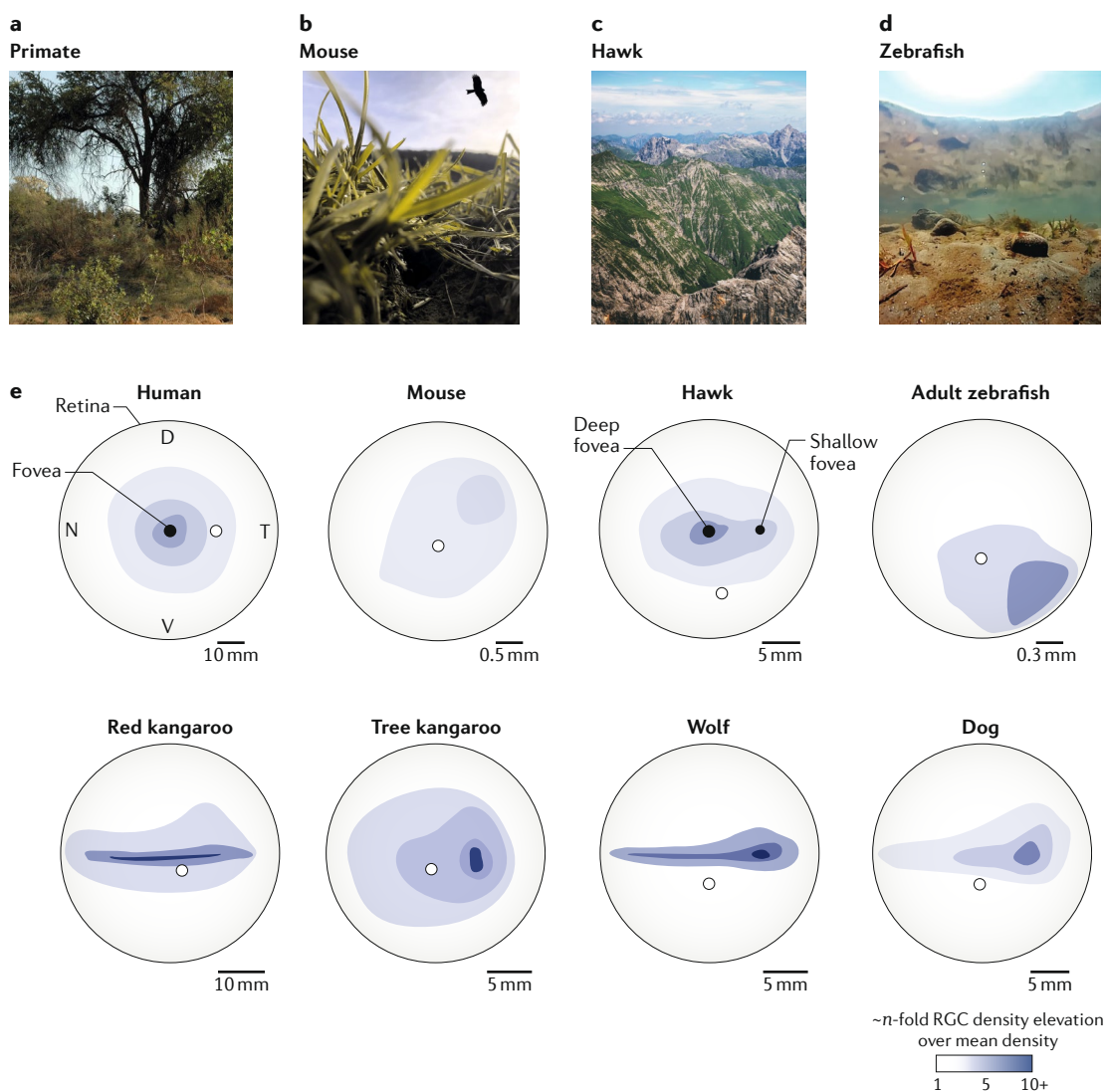


**Fig. 2 | Differential retinal ganglion cell topographies support vision in different visual environments. a–d |** Snapshots of the typical visual habitats of different animals. **e |** Representative retinal ganglion cell (RGC) density distributions across the whole retinas of different species. The schematics were created by our tracing published cell-count maps and subsequently using approximate graphical stitching to fit the images to a circular projection (human<sup>234</sup>, adult zebrafish<sup>198</sup>, hawk<sup>85</sup>, red kangaroo<sup>120</sup>, tree kangaroo<sup>120</sup>, wolf<sup>122</sup> and dog<sup>122</sup>). The schematic of the mouse retina was sketched by hand on the basis of data in REFS<sup>6,7,235</sup>. For each of the published maps, we identified a number of density 'contours', for each of which we estimated the total area and RGC density. We used this information to calculate the mean RGC density across the bulk of the retina. In each schematic, areas shaded in the lightest grey are those in which RGC density corresponded to this mean density, and regions with darker shading show approximate relative elevations above this mean. The densities shown in each region are approximate, having been estimated from RGC density schematics of flat-mounted retinas depicted in the original publications. The white circles indicate the position of the optic nerve head in each retina. The optics of the eye invert the incoming image, meaning that the dorsal retina (D) surveys the ground, while the ventral retina (V) surveys the sky. N, nasal, T, temporal. Part **a** is adapted, with permission, from the database as described in REF.<sup>167</sup>, Tkacik, G. et al., Natural images from the birthplace of the human eye. *PLoS ONE* **6**, e20409 (2011).



RGCs across species<sup>75</sup> (FIG. 2e). Acute zones are regions of the retina in which RGC density is higher than in the rest of the retina and a key feature of many vertebrate retinas: even mice may have one acute zone in the temporal retina<sup>101</sup> (but see REF.<sup>7</sup>), allowing them to somewhat oversample the visual space just in front of their nose. Importantly, even animals belonging to the same family can, when they live in different habitats, differ in the shape, location and extent of their acute zones. For example, animals living in open plains, such as the red kangaroo (*Macropus rufus*) or the arctic fox (*Alopex lagopus*), tend to feature a lengthy, horizontal streak of high RGC density that allows them to relatively oversample what is presumably the most important part of their visual world — the distant horizon<sup>119,120</sup>. In contrast, species that dwell in cluttered environments, such as forests that lack an obvious horizon — including the tree kangaroo (*Dendrolagus dorianus*) and the red fox (*Vulpes vulpes*) — instead usually have a spot-like RGC density distribution, dubbed ‘area centralis’<sup>119,120</sup>. These types of traits can evolve rapidly: wolves, for example, feature a pronounced horizontal streak leading into a dense area temporalis; however, dogs — following only some 15,000 years of domestication<sup>121</sup> — exhibit much less pronounced versions of this pattern<sup>101,119,122</sup> (FIG. 2e). Some species have more than one acute zone. For example, hippopotamuses, rhinoceroses and elephants have two to three acute zones, which have presumably evolved to compensate for their difficulty in rapidly turning their body and head<sup>89,123,124</sup>.

An acute zone is generally considered to be a fovea if there is additional structural rearrangement in the retinal circuits to more directly expose photoreceptors to incoming photons, thus limiting scatter and maximizing spatial acuity. Among mammals, only some primates (including humans) are foveated; however, foveas are also found in many birds and reptiles, as well as in some fish<sup>112,125,126</sup>. Some species, including many birds of prey, even have two foveas: a shallow fovea that is not unlike the human fovea and that is used when looking forward into potentially binocular space, and an even-higher-resolution deep fovea that is used when looking sideways (for example, to aid monocular object detection at a distance)<sup>127</sup> (FIG. 2e).

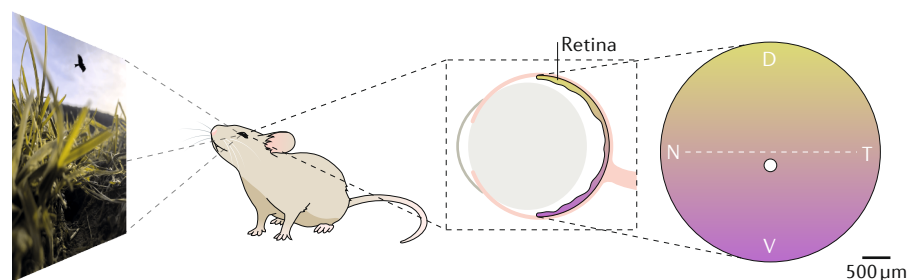
A consequence of the presence of visual acute zones is that the function of one part of the retina is not representative of the function of the entire eye. Here, a well-studied example is the primate fovea, in which the peripheral retina’s mix of rod and cone photoreceptor pathways is replaced by simplified circuits (the midget pathway)<sup>128</sup> in which there is a 1:1:1 connectivity between cones, bipolar cells and RGCs (reviewed in REF.<sup>37</sup>). The midget pathway also lacks substantial lateral interactions with inner retinal inhibitory circuits and is driven by cones that exhibit slower responses to light than their counterparts outside the fovea<sup>81</sup> (the latter is suggested to be an adaptation to cope with the high noise levels that invariably accompany its low-convergence connectivity<sup>80,81,129</sup>). In primates, this regional specialization is complemented by additional processing hardware beyond the retina: The rod-free centre of the fovea occupies only ~0.04% of the retinal surface (~2° visual angle) but a large percentage of the primary visual cortex

(V1) is dedicated to processing its output (giving a foveal magnification factor of ~8 mm/° at 1° eccentricity)<sup>130</sup>.

**Regional variability in retinal functional cell types.** Mice feature a wide range of retinal specializations associated with the vertical axis. Most famously, and in common with many other vertebrates (reviewed in REF.<sup>101</sup>), mice have a pronounced dorsoventral gradient in opsin expression across their cone photoreceptors<sup>131,132</sup>: cones expressing only the UV-sensitive S opsin (S cones) are sparse (~5%) and homogeneously distributed across the whole retina<sup>133</sup>; however, the ratio of S cones to the population of cones expressing the green-sensitive M opsin (M cones) changes along the dorsoventral axis of the retina, being M cone dominated in the dorsal retina and S cone dominated in the ventral retina (FIG. 3a). This renders the upper visual field strongly UV sensitive<sup>134</sup>. Furthermore, this retinal asymmetry is accompanied by a dorsal–ventral shift in the contrast sensitivity of the M cones from those responding in an approximately equal and opposite manner to light and dark stimuli to those preferring a dark stimulus<sup>6</sup>, potentially supporting aerial predator detection (see below; REF.<sup>117</sup>). Despite the S-cone dominance of the ventral retina, behavioural experiments indicate that mice can still discriminate colours with this part of the retina<sup>135</sup>, likely through a mechanism involving rod photoreceptor (green sensitive) versus S-cone opponency mediated by horizontal cells<sup>11,136</sup>.

Through genetic targeting, a large number of regional variations at the level of specific RGC types from the mouse retina’s established parts list have recently been reported<sup>7–9,136–138</sup> (FIG. 3b), suggesting that there may be regional adaptations of their upstream circuits. For example, the so-called alpha RGCs have been identified in many mammals and are some of the largest RGC types — in terms of both soma and dendritic arbour<sup>139</sup>. Different types of alpha RGCs seem to follow different regional patterns: those that display sustained responses to the onset or offset of light (‘sustained on’ and ‘sustained off’ alpha RGCs, respectively) have smaller dendritic fields and are denser in the dorsotemporal region of the retina than in other parts of the retina<sup>7</sup> (a difference that is predicted to affect spatial integration). By contrast, alpha RGCs that display a transient response to the light offset (‘transient off’ RGCs) are rather homogeneous in dendritic field size and distribution<sup>7</sup>; however, a change in their temporal response profile along the dorsoventral axis of the retina has been reported<sup>8</sup>. Another example is the JAM-B RGC, named after the transgenic marker line in which it was first described<sup>138</sup>. This RGC type has been reported to feature a strongly asymmetrical dendritic field morphology across most of the retina; however, in the ventral (and potentially the dorsal) periphery of the retina these RGCs become symmetrical<sup>138</sup>. JAM-B RGCs are orientation selective<sup>50</sup> as well as, under low-light conditions, direction selective<sup>136,138</sup> across most of the retina<sup>50</sup>; however, they become additionally colour opponent in the ventral retina<sup>136</sup>. Finally, complex patterns of regional specialization occur for classical direction-selective RGCs<sup>140</sup>: it has been reported that there is a systematic tilt in the preferred motion direction of these cells that depends on their retinal

# a Spectral sensitivity across the retina



# b Selected RGC subtypes across the retina

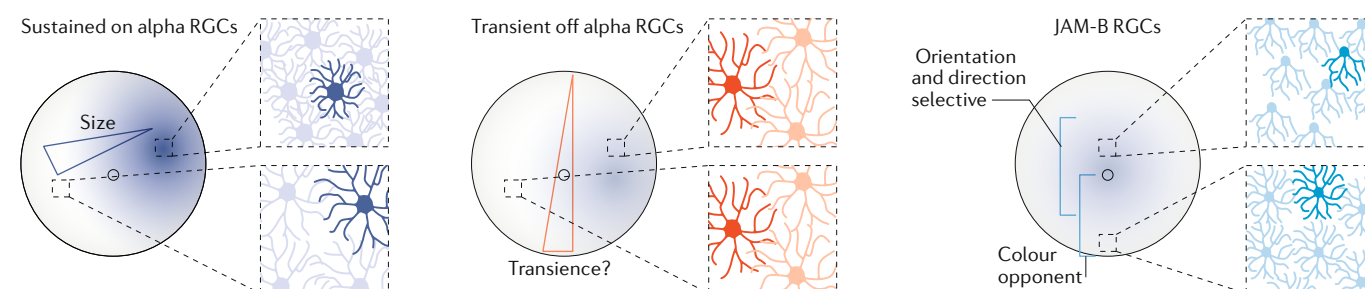


**Fig. 3 | Specializations of retinal neurons across the retina. a** The differential distribution of cone photoreceptor opsins along the dorsoventral axis of the mouse retina. Green shading indicates the approximate density of green-sensitive M cones, which dominate the ground-observing dorsal retina, and lilac shading indicates the approximate density of UV-sensitive S cones, which dominate the sky-observing ventral retina (based on data in REFS<sup>6,132,236</sup>). **b** Examples of variations in the properties of three different types of mouse retinal ganglion cell (RGC). Their schematic morphology and tiling (mosaic) properties in two representative regions are indicated in the inset boxes and additional regionally changing properties are also illustrated. Following a nasoventral dorsotemporal gradient, sustained on alpha RGCs increase their density while decreasing their dendritic field size<sup>7</sup>, but their temporal response profile remains largely unchanged. Transient off alpha RGCs, by contrast, are rather homogeneous in dendritic field size and distribution<sup>7</sup>, but have been reported to change their temporal properties along the dorsoventral axis: specifically, their responses are more transient in the ventral retina<sup>8</sup>. JAM-B cells have been reported to feature an asymmetrical morphology in most of the retina but become symmetrical in the ventral (and possibly in the dorsal) periphery<sup>138</sup>. They have been reported to be direction selective under low-light conditions<sup>50,136</sup> as well as orientation selective<sup>50</sup> across the retina (except for the dorsal and ventral periphery), and to become colour opponent in the ventral retina<sup>136</sup>.

location, which allows them to align and respond better to self-motion flow fields associated with self-motion and eye motion<sup>9</sup>. This is reminiscent of the local motion sensitivities of tangential neurons in flying insects, which exhibit complex receptive fields that directly reflect the distribution of local motion signals on the animal's eye during self-motion<sup>141</sup>. It is likely that more regionalization patterns exist in mice; however, it is at times difficult to disentangle true regional specializations from artefacts resulting from regionally restricted transgene expression patterns. For instance, so-called W3 RGCs, which detect small dark moving objects<sup>56</sup>, have been reported to be much denser in the medioventral retina than in the rest of the retina. However, these W3 RGCs are only one of several RGC subpopulations that are labelled in this transgenic mouse line, and it is therefore still unclear to what extent the high medioventral density of labelled RGCs can be attributed to a concentration of this cell type versus differential transgene expression<sup>55</sup>.

While we have some knowledge of functional asymmetries at the level of the retina's input (photoreceptors) and its output (RGCs), we are only just beginning to build an understanding of regional variations in the cell

types that mediate the steps in between<sup>142</sup>. Here, work in larval zebrafish shows that functional inhomogeneities across the retinal surface can be rather pronounced. In this tiny animal, both the anatomy and the function of bipolar cells vary substantially across the retina<sup>3</sup>. Because there is little chromatic information available directly above the animal, it appears that larval zebrafish invest in achromatic silhouette detection circuits over colour-opponent ones in the ventral retina. In contrast, the natural horizon is colour-rich and, in response, the retinal horizon features multiple colour-opponent bipolar cell circuits alongside a near doubling of the inner retina's thickness. In addition, the region of the retina receiving input from the visual space just above the horizon and in front of the animal is heavily dominated by specialized UV-sensitive cone photoreceptors and inner retinal UV-on circuits, which is likely to support visually guided prey capture of UV-bright plankton<sup>3,10</sup>.

From the findings taken together, it is clear that retinal circuits and neuron types vary in anatomy and function across the retinal surface. This is in contrast to the traditional view that a neuron type that tiles the retina regularly also exhibits one stereotyped (though

## Power spectrum

A representation of the energy in each of the frequency components in an image. It can be computed using a Fourier transform.

## Linear model

A model in which neurons exclusively perform linear operations such as forming weighted sums of inputs, without any non-linearities, such as thresholding.

## Cost function

A mathematical function that assigns a cost to a state of the world, an action or a representation and therefore measures its quality. Examples include the mean squared error, which measures how well the representation of an image would allow it to be reconstructed.

potentially size-scaled) morphology and one function<sup>26,143,144</sup>. In the end, irrespective of whether it is shown that these properties all systematically vary across the retinal surface, it seems likely that our growing understanding of the structure and function of the retina's neuronal building blocks will continue to be central to the ongoing debate on neuron typing across the brain<sup>144</sup>.

## Linking retinal diversity to behaviour

How can differences between species in the complement of retinal cell types or in regional retinal specializations be related to the natural visual environment inhabited by different animals and their strategies to view the world? On an intuitive level, one may argue that the anisotropy in cone opsin distribution in the mouse retina may reflect an adaptation to the distinct contrast distributions in the sky and on the ground, improving the mouse's ability to detect aerial predators (usually dark moving objects against the sky)<sup>6</sup>. Likewise, the potentially higher density of W3 RGCs in the upward-looking ventral retina<sup>56</sup>, coupled with this RGC type's preference for small dark objects moving on a bright background<sup>56</sup>, makes it tempting to speculate that there is an early warning system located in the ventral retina and roughly tuned to the silhouettes of predatory birds<sup>117</sup> (but see earlier).

Still, it is often difficult to convincingly link functional local adaptations to properties of the natural environment, even when the link to the natural habitat and behaviour seems obvious, because there is always danger of oversimplification. For instance, the aforementioned W3 RGCs would presumably also respond to a wide range of harmless stimuli such as wind-driven movements in overhanging branches. Alternatively, we can attempt to go beyond such 'word models' and instead try to quantitatively link the properties of retinal neurons in different animals to the statistics of their respective natural environments and a mathematically precise formulation of their ecological necessities.

The quest for a quantitative theory of the retina's purpose has fascinated researchers for many years. Several theories have been proposed that try to explain the physiology of retinal neurons from statistical properties of the natural environment of the animal<sup>15,16,145,146</sup>. In the natural environment, there are strong correlations between the spatial and temporal features of typical visual scenes, as well as in their spectral composition. These correlations in photographs of natural scenes can be seen in the typical  $1/f$  power spectrum, where low spatial frequencies have more power than high spatial frequencies<sup>147,148</sup>. The classical efficient coding theory suggests that one purpose of the retina is to find the least redundant representation of the visual input by 'whitening' the power spectrum, which is equivalent to removing the spatial correlations. This ensures that the relevant visual information can be effectively transferred over the bottleneck that the optic nerve represents<sup>16,145,147,149</sup>.

This theory offers a solid theoretical account of various properties of retinal circuits: For example, one can show mathematically that whitening of the power spectrum can be achieved by elliptical centre-surround receptive fields, suggesting that this feature of many retinal neurons may have evolved to provide an efficient

representation of visual scenes<sup>149</sup>. It even predicts the red-green and blue-yellow antagonism found in colour-opponent RGCs in primates, showing that these cells are ideally suited to decorrelate the colour space of natural visual scenes<sup>105</sup>. Beyond the general organization of receptive field structure, the efficient coding hypothesis has also provided accurate accounts of the fine mosaic structure of RGC receptive fields in the primate retina<sup>150</sup>. Finally, retinal non-linearities such as those that allow adaptation to natural scene statistics have been linked to efficient coding<sup>151,152</sup>.

Nonetheless, from a theoretical viewpoint the retina remains far from solved. Perhaps the most obvious mismatch between experimental observations and theory is a numerical one: primates have on the order of 20 distinct RGC types<sup>80,153</sup> and mice have at least 40 (REFS<sup>44,49,154</sup>). These cells have been shown to have a wide range of computational properties<sup>49</sup>, yet efficient coding theory typically accounts for only a small number of simple centre-surround types of RGCs. To what extent can the emergence of this multitude of different RGC types be accounted for by theory? The first steps towards this goal have been taken. For example, it has been shown that splitting the visual signal into on and off channels aids signal coding<sup>155</sup>. In addition, the emergence of a few specific RGC types with different spatio-temporal characteristics has been explained in terms of efficient coding<sup>156,157</sup>. Extending the simple linear model of efficient coding to a neural network model including non-linearities reveals an optimal encoding scheme in which there are four cell types, matched in two on and off pairs with different spatial characteristics, resembling primate midget and parasol RGCs<sup>157</sup> (FIG. 4a).

To what extent the diversity of retinal cell types will ever be explained by a unifying theory is an open question. It is probably naive to believe that simply plugging videos capturing the natural environment of a species into a model or theory alone will ever yield a precise account of all the receptive field properties of the species' RGC types, as the latter will also require a careful account of the species' behavioural demands and necessities for survival. However, ideas about the specific feature channels that might encode survival-critical information have been much harder to make quantitatively precise<sup>16,74,158</sup>.

Use of deep neural networks as task-driven models of the visual system may offer an interesting way to formalize these notions (reviewed in REF<sup>159</sup>). For example, in the case of the ventrotemporal retina's UV dominance in larval zebrafish<sup>3,10</sup>, simply considering the statistical frequency of UV light in the visual field will not account for the neural response properties — for this, we need to know about the behavioural interest of the larvae in UV-scattering prey (that is, the task). If the UV scatter were just a nuisance, the retina might do well to discard it early on to avoid wasting costly resources in representing it. Thus, part of any theory would need to account for ecological demands of a species. Possibly, this could be encoded in the cost function that we might assume the retina to solve optimally. Thus, extending classical notions by formally encoding behavioural necessities may provide a viable path forward to reconcile the finding of many RGC types with theory.

Predictions of efficient coding have often been formulated on the descriptive level of cellular properties such as receptive field structure but have provided few constraints on the implementation level. For example, many RGCs do not simply implement their receptive field by pooling inputs, but instead show non-linear centre-surround interactions<sup>160</sup> (FIG. 4b) through circuits that, in turn, consist of non-linearly integrated subunits<sup>161–163</sup>

(FIG. 4c). Indeed, a recent study and preliminary findings have shown that taking this subunit structure into account can markedly improve the predictions of statistical RGC models in response to artificial and natural stimuli<sup>14,164</sup> (FIG. 4d,e). Also, three-layer deep neural network models inspired by retinal circuits currently yield the best predictions of neural activity at the RGC level and provide non-trivial predictions for other properties of retinal

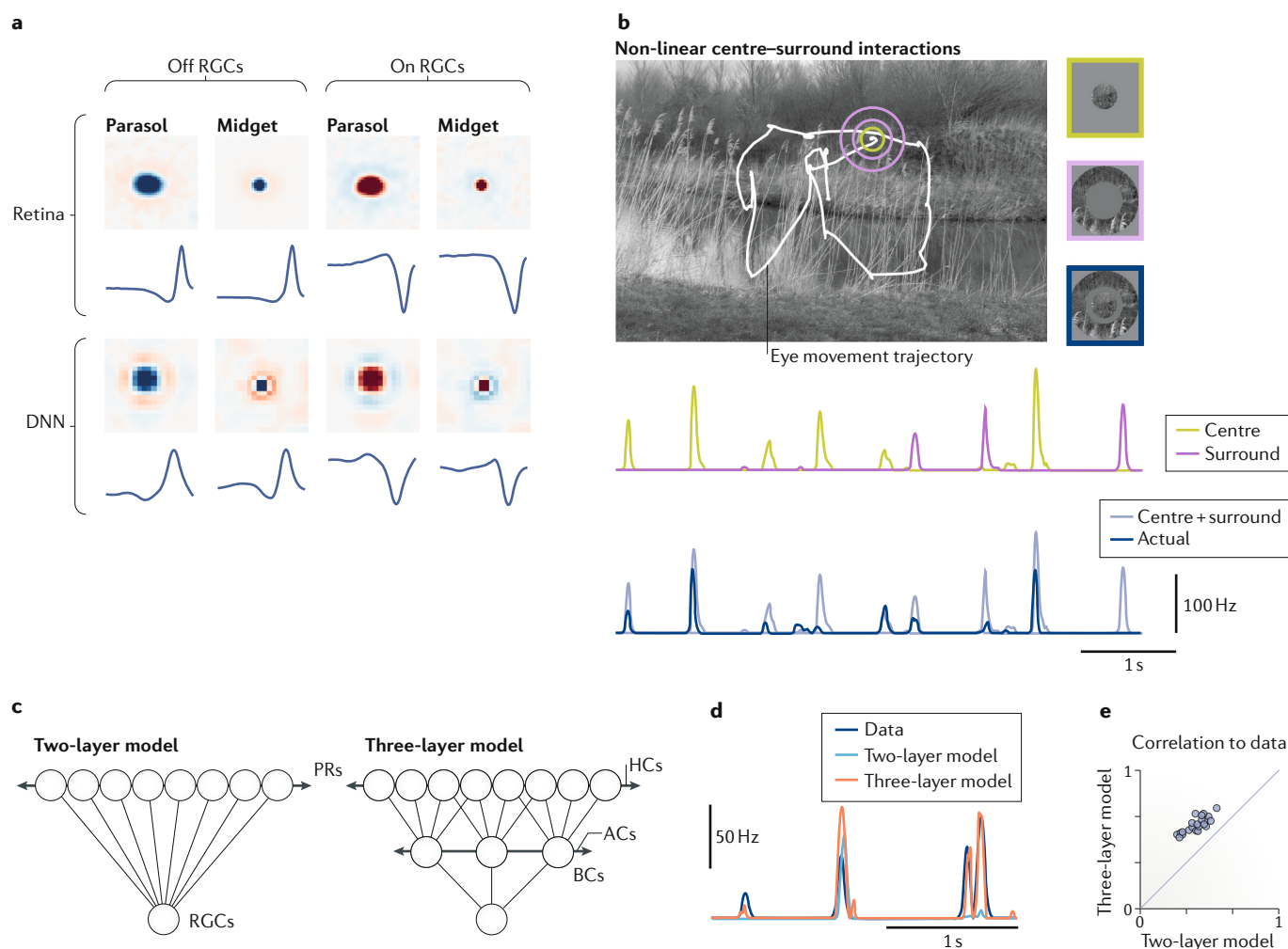


**Fig. 4 | Theoretical accounts of retinal designs. a** | A deep neural network (DNN) model with fixed firing rate budget reveals an optimal encoding scheme with four cell types with properties reminiscent of primate midget and parasol retinal ganglion cell (RGC) types. The top panel shows spatial and temporal receptive fields of off (left) and on (right) parasol (large) and midget (small) RGCs computed from spiking data measured in primate retina. The bottom panel shows spatial and temporal receptive fields of the four cell types found in the DNN model. **b** | When presented with natural scene data, RGC centre-surround interactions can be highly non-linear<sup>160</sup>. The top panel shows a natural scene with a macaque's eye movement trajectory indicated in white. The boxes to the right show examples of single-frame centre (green), surround (purple) and centre-surround (black) stimuli extracted from the same part of this scene, as seen by a model RGC. Upper traces show responses measured from an example RGC in the macaque retina when presented with the centre-only (green) and surround-only (purple) stimuli. The lower trace shows that the sum of the independently measured centre and surround responses (grey) overestimates the measured response when centre and surround stimuli are presented simultaneously (black). **c** | Examples of two-layer and three-layer models of retinal

processing. Circles and lines indicate nodes (photoreceptors (PRs), bipolar cells (BCs) and RGCs) and the connections between them (synapses), respectively. Arrows indicate the direction of connectivity via within-layer inhibitory networks (horizontal cells (HCs) between PRs and amacrine cells (ACs) between BCs). Two-layer networks typically seek to explain RGC responses on the basis of functional connections to PRs alone. In contrast, three-layer networks include BCs to form internal subunits. Both at the PR stage and the BC stage, lateral interactions via HCs and ACs, respectively, can be included to increase model accuracy. Three-layer networks can often outperform two-layer networks when aiming to model responses to complex or natural stimuli<sup>161,164,166,237</sup>. **d,e** | Two- and three-layer models were used to fit measured tiger salamander RGC responses to a complex stimulus (part d). The three-layer model consistently outperformed the two-layer model, as quantified in the correlation coefficient of each model prediction to the measured data (part e). Part a was modified with permission from REF.<sup>157</sup>, Neural Information Processing System. Part b was modified with permission from REF.<sup>160</sup>, CC-BY-4.0, <https://creativecommons.org/licenses/by/4.0/>. Parts d and e were modified with permission from REF.<sup>166</sup>, CC-BY-4.0, <https://creativecommons.org/licenses/by/4.0/>.



## Box 3 | A non-exhaustive list of open questions

- To what extent is the strongly elevated density of retinal neurons in some species, such as many birds, related to higher spatial acuity as opposed to the presence of additional circuits for potentially novel computations? If the latter, what are those computations?
- Do foveated non-primate vertebrates have a primate-like 1:1:1 midget pathway?
- Do direction-selective circuits across species draw on the same cellular and synaptic hardware in all species? Do ancient vertebrates such as lampreys or sharks have mammalian like direction-selective circuits?
- Is the presence of orientation selectivity in cells upstream of retinal ganglion cells in larval zebrafish a general phenomenon? What other computations typically thought of as being unique to retinal ganglion cells can be performed earlier in the network? Is computational 'front-loading' related to phylogeny and/or eye size?
- Do all retinal neurons vary in some way across the retinal surface?
- To what extent can the computational complement of output channels of any one species be explained by its visuoecological niche and behavioural demands? Alternatively, can a description of a given visuoecological niche quantitatively predict how a given retina is functionally organized?
- What is the full extent of neuromodulatory influences on retinal function in vivo, and how are key neuromodulatory circuits controlled?

circuits<sup>165,166</sup>. Thus, developing theoretical accounts of retinal function which allow constraints to be placed on the necessary building blocks on the mechanistic level is an additional avenue for future research.

Finally, to return to our original question, the theory of efficient coding has rarely been used to derive experimentally testable predictions about retinal specializations in different species or parts of the retina (as discussed in REFS<sup>3,7,8,56</sup>). The recent publication of several datasets consisting of images and movies that mimic the natural statistics of the environment of different species will likely facilitate such work<sup>3,167–169</sup>. For example, these datasets could be used to ask whether a theory can predict quantitatively the differences in the response properties of cells located across the retina of a given species. Alternatively, they could be used to ask whether a theory can predict differences and similarities in the complement of RGC types found in different species, on the basis of differences in their natural environment. It is likely that, in addition to efficient coding constraints, such a future theory of early visual processing would need to consider the ecological demands of a species in order to make realistic predictions. The plethora of experimental data that are becoming available would provide strong tests of any such theory.

### Outlook

We have seen that the structure and function of retinal circuits profoundly vary both between species and between different regions across the retina of a single species. Indeed, further variations exist within

retinal regions across the time of day or even seasons (Supplementary Box 1). Accordingly, to understand our own sense of vision and to study biological solutions to vision in a more general sense, it will be critical to (re-) expand our currently narrow focus on but a handful of models and often non-naturalistic experimental conditions. Only a representative cross section across all these levels can guide our understanding of which (if any) circuit motifs and computational solutions are broadly conserved, which are unique solutions that apply to only a narrow set of circumstances and how retinal circuits can switch between them on physiological and evolutionary timescales (BOX 3).

In particular, we suggest that expanding work on birds, which in many ways are the pinnacle of vertebrate retinal complexity, might aid our understanding of what retinal circuits — and thus neuronal networks — can achieve if pushed to the limit. Similarly, pursuing some of the long-standing questions raised in the classical literature on amphibians might greatly enrich our understanding of retinal organization in a more general sense. For example, how directly can the activity of single or small groups of RGCs alone trigger complex behaviour, as implied for the 'bug detectors' that Lettvin described in the frog retina<sup>74</sup>?

In parallel, it will be important to build additional depth in our understanding of species that are already well studied, to further delineate how their circuits vary in retinal space and circadian/seasonal time. A possible focus might be the inner retina<sup>142</sup>, the regional specializations of which remain scarcely explored even in mice. In aid of in-depth circuit comparisons, it will be important to simultaneously boost work on at least one or two additional species to eventually attain a level of understanding similar to that currently held for mice. Promising candidates include non-human primates (because their eyes are similar to those of humans) and zebrafish (for their ease of experimental access, the large body of existing literature and their distant phylogenetic relation to mammals). Any such efforts are set to immensely benefit from current high-throughput tools for mapping neuronal structure, function and gene expression.

Ultimately, retinal circuits evolved to operate in the live, behaving animal as it responds to changes in its visual environment and internal state on timescales from milliseconds to seasons<sup>170</sup>. Understanding how these factors play into the flexibility and design of retinal circuits in vivo will require direct, and ideally unperturbed, measurements of retinal structure and function over long timescales alongside reversible experimental manipulations at the circuit level.

Published online: 28 November 2019

1. Land, M. F. & Nilsson, D.-E. *Animal Eyes* (Oxford Univ. Press, 2012).
2. Cronin, T. W., Johnsen, S., Marshall, N. J. & Warrant, E. J. *Visual Ecology* (Princeton Univ. Press, 2014).
3. Zimmermann, M. J. Y. et al. Zebrafish differentially process color across visual space to match natural scenes. *Curr. Biol.* **28**, 2018–2032 (2018).  
**A study on larval zebrafish showing how the function of inner retinal circuits varies considerably across the eye to meet natural demands.**

4. Turner, M. H. & Rieke, F. Synaptic rectification controls nonlinear spatial integration of natural visual inputs. *Neuron* **90**, 1257–1271 (2016).
5. Kühn, N. K. & Golisch, T. Activity correlations between direction-selective retinal ganglion cells synergistically enhance motion decoding from complex visual scenes. *Neuron* **101**, 963–976 (2019).
6. Baden, T. et al. A tale of two retinal domains: near-optimal sampling of achromatic contrasts in natural

7. scenes through asymmetric photoreceptor distribution. *Neuron* **80**, 1206–1217 (2013).
7. Bleckert, A., Schwartz, G. W., Turner, M. H., Rieke, F. & Wong, R. O. L. Visual space is represented by nonmatching topographies of distinct mouse retinal ganglion cell types. *Curr. Biol.* **24**, 310–315 (2014).  
**A study on mice showing that several types of RGCs exhibit distinct properties depending on their position on the retina.**

8. Warwick, R. A., Kaushansky, N., Sarid, N., Golan, A. & Rivlin-Etzion, M. Inhomogeneous encoding of the visual field in the mouse retina. *Curr. Biol.* **28**, 655–665 (2018).
9. Sabbah, S. et al. A retinal code for motion along the gravitational and body axes. *Nature* **546**, 492–497 (2017).
10. Yoshimatsu, T., Schröder, C., Berens, P. & Baden, T. Cellular and molecular mechanisms of photoreceptor tuning for prey capture in larval zebrafish. Preprint at *bioRxiv* <https://doi.org/10.1101/744615> (2019).
11. Szatko, K. P. et al. Neural circuits in the mouse retina support color vision in the upper visual field. Preprint at *bioRxiv* <https://doi.org/10.1101/745539> (2019).
12. Dehmelt, F. A. et al. Spherical arena reveals optokinetic response tuning to stimulus location, size and frequency across entire visual field of larval zebrafish. Preprint at *bioRxiv* <https://doi.org/10.1101/754408> (2019).
13. Heitman, A. et al. Testing pseudo-linear models of responses to natural scenes in primate retina. Preprint at *bioRxiv* <https://doi.org/10.1101/045336> (2016).
14. Shah, N. P. et al. Inference of nonlinear spatial subunits by spike-triggered clustering in primate retina. Preprint at *bioRxiv* <https://doi.org/10.1101/496422> (2018).
15. Attneave, F. Some informational aspects of visual perception. *Psychol. Rev.* **61**, 183–193 (1954).
16. Barlow, H. B. in *Sensory Communication* Ch. 13 (ed. Rosenblith, W. A.) (MIT Press, 1961).
17. Wässle, H. Parallel processing in the mammalian retina. *Nat. Rev. Neurosci.* **5**, 747–757 (2004).
18. Masland, R. H. The neuronal organization of the retina. *Neuron* **76**, 266–280 (2012).
19. Chapot, C. A., Euler, T. & Schubert, T. How do horizontal cells ‘talk’ to cone photoreceptors? Different levels of complexity at the cone-horizontal cell synapse. *J. Physiol.* **595**, 5495–5506 (2017).
20. Thoreson, W. B. & Mangel, S. C. Lateral interactions in the outer retina. *Prog. Retin. Eye Res.* **31**, 407–441 (2012).
21. Euler, T. T., Haverkamp, S. S., Schubert, T. T. & Baden, T. Retinal bipolar cells: elementary building blocks of vision. *Nat. Rev. Neurosci.* **15**, 507–519 (2014).
22. Masland, R. H. The tasks of amacrine cells. *Vis. Neurosci.* **29**, 3–9 (2012).
23. Franke, K. & Baden, T. General features of inhibition in the inner retina. *J. Physiol.* **595**, 5507–5515 (2017).
24. Baccus, S. A. Timing and computation in inner retinal circuitry. *Annu. Rev. Physiol.* **69**, 271–290 (2007).
25. Diamond, J. S. Inhibitory interneurons in the retina: types, circuitry, and function. *Annu. Rev. Vis. Sci.* **3**, 1–24 (2017).
26. Sanes, J. R. & Masland, R. H. The types of retinal ganglion cells: current status and implications for neuronal classification. *Annu. Rev. Neurosci.* **38**, 221–246 (2014).
27. Dhande, O. S. & Huberman, A. D. Retinal ganglion cell maps in the brain: implications for visual processing. *Curr. Opin. Neurobiol.* **24**, 133–142 (2014).
28. Kuffler, S. W. Discharge patterns and functional organization of mammalian retina. *J. Neurophysiol.* **16**, 37–68 (1953).
29. Protti, Da, Flores-Herr, N. & von Gersdorff, H. Light evokes Ca<sup>2+</sup> spikes in the axon terminal of a retinal bipolar cell. *Neuron* **25**, 215–227 (2000).
30. Baden, T., Esposti, F., Nikolaev, A. & Lagnado, L. Spikes in retinal bipolar cells phase-lock to visual stimuli with millisecond precision. *Curr. Biol.* **21**, 1859–1869 (2011).
31. Baden, T., Berens, P., Bethge, M. & Euler, T. Spikes in mammalian bipolar cells support temporal layering of the inner retina. *Curr. Biol.* **23**, 48–52 (2012).
32. Puthussery, T., Venkataramani, S., Gayet-Primo, J., Smith, R. G. & Taylor, W. R. NaV1.1 channels in axon initial segments of bipolar cells augment input to magnocellular visual pathways in the primate retina. *J. Neurosci.* **33**, 16045–16059 (2013).
33. Saszik, S. & DeVries, S. H. A mammalian retinal bipolar cell uses both graded changes in membrane voltage and all-or-nothing Na<sup>+</sup> spikes to encode light. *J. Neurosci.* **32**, 297–307 (2012).
34. Franke, K. et al. Inhibition decorrelates visual feature representations in the inner retina. *Nature* **542**, 439–444 (2017).
35. James, B., Darnet, L., Moya-Díaz, J., Seibel, S.-H. & Lagnado, L. An amplitude code transmits information at a visual synapse. *Nat. Neurosci.* **22**, 1140–1147 (2019).
36. Baden, T., Euler, T., Weckström, M. & Lagnado, L. Spikes and ribbon synapses in early vision. *Trends Neurosci.* **36**, 480–488 (2013).
37. Baden, T., Schubert, T., Berens, P. & Euler, T. The functional organization of vertebrate retinal circuits for vision. *Oxford Res. Encycl. Neurosci.* <https://doi.org/10.1093/acrefore/9780190264086.013.68> (2018).
38. Bloomfield, S. A. & Dacheux, R. F. Rod vision: pathways and processing in the mammalian retina. *Prog. Retin. Eye Res.* **20**, 351–384 (2001).
39. Mauss, A. S., Vlasits, A., Borst, A. & Feller, M. Visual circuits for direction selectivity. *Annu. Rev. Neurosci.* **40**, 211–230 (2017).
40. Wässle, H., Puller, C., Müller, F. & Haverkamp, S. Cone contacts, mosaics, and territories of bipolar cells in the mouse retina. *J. Neurosci.* **29**, 106–117 (2009).
41. Breuninger, T., Puller, C., Haverkamp, S. & Euler, T. Chromatic bipolar cell pathways in the mouse retina. *J. Neurosci.* **31**, 6504–6517 (2011).
42. Sun, W., Li, N. & He, S. Large-scale morphological survey of mouse retinal ganglion cells. *J. Comp. Neurol.* **451**, 115–126 (2002).
43. Völgyi, B., Chheda, S. & Bloomfield, S. A. Tracer coupling patterns of the ganglion cell subtypes in the mouse retina. *J. Comp. Neurol.* **512**, 664–687 (2009).
44. Bae, J. A. et al. Digital museum of retinal ganglion cells with dense anatomy and physiology. *Cell* **173**, 1293–1306 (2018).
45. Serial section electron microscopy level anatomical classification of RGCs in the mouse.
46. Behrens, C. et al. Connectivity map of bipolar cells and photoreceptors in the mouse retina. *eLife* **5**, 1206–1217 (2016).
47. Kim, J. S. et al. Space–time wiring specificity supports direction selectivity in the retina. *Nature* **509**, 331–336 (2014).
48. Helmstaedter, M. et al. Connectomic reconstruction of the inner plexiform layer in the mouse retina. *Nature* **500**, 168–174 (2013).
49. Borst, A. & Euler, T. Seeing things in motion: models, circuits, and mechanisms. *Neuron* **71**, 974–994 (2011).
50. Baden, T. et al. The functional diversity of retinal ganglion cells in the mouse. *Nature* **529**, 345–350 (2016).
51. Large-scale functional account of RGCs in the mouse.
52. Nath, A. & Schwartz, G. W. Cardinal orientation selectivity is represented by two distinct ganglion cell types in mouse retina. *J. Neurosci.* **36**, 3208–3221 (2016).
53. Venkataramani, S. & Taylor, W. R. Orientation selectivity in rabbit retinal ganglion cells is mediated by presynaptic inhibition. *J. Neurosci.* **30**, 15664–15676 (2010).
54. Venkataramani, S. & Taylor, W. R. Synaptic mechanisms generating orientation selectivity in the ON pathway of the rabbit retina. *J. Neurosci.* **36**, 3336–3349 (2016).
55. Nath, A. & Schwartz, G. W. Electrical synapses convey orientation selectivity in the mouse retina. *Nat. Commun.* **8**, 2025 (2017).
56. Krieger, B., Qiao, M., Rouso, D. L., Sanes, J. R. & Meister, M. Four alpha ganglion cell types in mouse retina: Function, structure, and molecular signatures. *PLOS ONE* **12**, e0180091 (2017).
57. Jacoby, J. & Schwartz, G. W. Three small-receptive-field ganglion cells in the mouse retina are distinctly tuned to size, speed, and object motion. *J. Neurosci.* **37**, 610–625 (2017).
58. A study on mice describing the anatomy and function of three distinct small-field RGCs in the mouse.
59. Zhang, Y., Kim, I.-J., Sanes, J. R. & Meister, M. The most numerous ganglion cell type of the mouse retina is a selective feature detector. *Proc. Natl Acad. Sci. USA* **109**, E2391–E2398 (2012).
60. Mani, A. & Schwartz, G. W. Circuit mechanism of a novel retinal ganglion cell with non-canonical receptive field structure. *Curr. Biol.* **27**, 471–482 (2017).
61. Munch, T. A. et al. Approach sensitivity in the retina processed by a multifunctional neural circuit. *Nat. Neurosci.* **12**, 1308–1316 (2009).
62. Jacoby, J. & Schwartz, G. W. Typology and circuitry of suppressed-by-contrast retinal ganglion cells. *Front. Cell. Neurosci.* **12**, 269 (2018).
63. Sivyer, B., Taylor, W. R. & Vaney, D. I. Uniformity detector retinal ganglion cells fire complex spikes and receive only light-evoked inhibition. *Proc. Natl Acad. Sci. USA* **107**, 5628–5633 (2010).
64. Lazzarini Ospri, L., Prusky, G. & Hattar, S. Mood, the circadian system, and melanopsin retinal ganglion cells. *Annu. Rev. Neurosci.* **40**, 539–556 (2017).
65. Demb, J. B. & Singer, J. H. Intrinsic properties and functional circuitry of the All amacrine cell. *Vis. Neurosci.* **29**, 51–60 (2012).
66. Grimes, W. N., Zhang, J., Graydon, C. W., Kachar, B. & Diamond, J. S. Retinal parallel processors: more than 100 independent microcircuits operate within a single interneuron. *Neuron* **65**, 873–885 (2010).
67. Haverkamp, S., Wässle, H. & Wässle, H. Characterization of an amacrine cell type of the mammalian retina immunoreactive for vesicular glutamate transporter 3. *J. Comp. Neurol.* **468**, 251–263 (2004).
68. Lee, S. et al. An unconventional glutamatergic circuit in the retina formed by vGluT3 amacrine cells. *Neuron* **84**, 708–715 (2014).
69. Kim, T., Soto, F. & Kerschensteiner, D. An excitatory amacrine cell detects object motion and provides feature-selective input to ganglion cells in the mouse retina. *eLife* **4**, e08025 (2015).
70. Lee, S. et al. Segregated glycine–glutamate co-transmission from vGluT3 amacrine cells to contrast-suppressed and contrast-enhanced retinal circuits. *Neuron* **90**, 27–34 (2016).
71. Masland, R. H. & Martin, P. R. The unsolved mystery of vision. *Curr. Biol.* **17**, 577–582 (2007).
72. Ramón y Cajal, S. La rétine des vertébrés [French]. *La Cellule* **9**, 119–257 (1893).
73. Wang, J., Jacoby, R. & Wu, S. M. Physiological and morphological characterization of ganglion cells in the salamander retina. *Vis. Res.* **119**, 60–72 (2016).
74. Lisney, T. J., Wylie, D. R., Kolominsky, J. & Iwaniuk, A. N. Eye morphology and retinal topography in hummingbirds (Trochilidae: Aves). *Brain Behav. Evol.* **86**, 176–190 (2015).
75. Anatomical study on RGCs in the retinas of avian retinal organization in general.
76. Mitkus, M., Nevitt, G. A., Danielsen, J. & Kelber, A. Vision on the high seas: spatial resolution and optical sensitivity in two procellariiform seabirds with different foraging strategies. *J. Exp. Biol.* **219**, 3329–3338 (2016).
77. Potier, S., Mitkus, M. & Kelber, A. High resolution of colour vision, but low contrast sensitivity in a diurnal raptor. *Proc. R. Soc. Lond. B Biol. Sci.* **29**, 1885 (2018).
78. Lettvin, J., Maturana, H., McCulloch, W. & Pitts, W. What the frog’s eye tells the frog’s brain. *Proc. IRE* **47**, 1940–1951 (1959).
79. Landmark article coining the idea that RGCs might be highly task specific. Put forward the notion of ‘bug detectors’.
80. Collin, S. P. A web-based archive for topographic maps of retinal cell distribution in vertebrates: invited paper. *Clin. Exp. Optom.* **91**, 85–95 (2008).
81. Mikelberg, F. S., Drance, S. M., Schulzer, M., Yidegiligne, H. M. & Weis, M. M. The normal human optic nerve: axon count and axon diameter distribution. *Ophthalmology* **96**, 1325–1328 (1989).
82. Jeon, C. J., Strettoi, E. & Masland, R. H. The major cell populations of the mouse retina. *J. Neurosci.* **18**, 8936–8946 (1998).
83. Johnston, J. & Lagnado, L. What the fish’s eye tells the fish’s brain. *Neuron* **76**, 257–259 (2012).
84. Montgomery, G. How we see things that move. in *Seeing, Hearing and Smelling the World*. (Howard Hughes Medical Institute, 1995).
85. Peng, Y.-R. et al. Molecular classification and comparative taxonomics of foveal and peripheral cells in primate retina. *Cell* **176**, 1222–1237 (2019).
86. Study in primates demonstrating that foveal and peripheral circuits are molecularly distinct.
87. Sinha, R. et al. Cellular and circuit mechanisms shaping the perceptual properties of the primate fovea. *Cell* **168**, 413–426 (2017).
88. Study in primates exploring region-specific functional circuit motifs of the primate fovea.
89. Easter, Jr. S. S. & Nicola, G. N. The development of vision in the zebrafish (*Danio rerio*). *Dev. Biol.* **180**, 646–663 (1996).
90. Li, Y. N., Tsujimura, T., Kawamura, S. & Dowling, J. E. Bipolar cell-photoreceptor connectivity in the zebrafish (*Danio rerio*) retina. *J. Comp. Neurol.* **520**, 3786–3802 (2012).
91. Lindsey, J., Ocko, S. A., Ganguli, S. & Deny, S. A unified theory of early visual representations from retina to cortex through anatomically constrained deep CNNs. In *Proceedings of Seventh International Conference on Learning Representations (ICLR, 2019)*.
92. Inzunza, O., Bravo, H., Smith, R. L. & Angel, M. Topography and morphology of retinal ganglion cells in Falconiforms: a study on predatory and carrion-eating birds. *Anat. Rec.* **229**, 271–277 (1991).

86. Bousfield, J. D. & Pessoa, V. F. Changes in ganglion cell density during post-metamorphic development in a neotropical tree frog *Hyla raniceps*. *Vis. Res.* **20**, 501–510 (1980).
87. Lisney, T. J. & Collin, S. P. Retinal ganglion cell distribution and spatial resolving power in elasmobranchs. *Brain Behav. Evol.* **72**, 59–77 (2008).
88. Ding, H., Smith, R. G., Poleg-Polsky, A., Diamond, J. S. & Briggman, K. L. Species-specific wiring for direction selectivity in the mammalian retina. *Nature* **535**, 105–110 (2016).  
**Study on mice and rabbits demonstrating that in these species retinal circuits for direction selectivity use distinct dendritic wiring motifs to acknowledge differences in eye sizes.**
89. Pettigrew, J. D., Bhagwandani, A., Haagen, M. & Manger, P. R. Visual acuity and heterogeneities of retinal ganglion cell densities and the tapetum lucidum of the African elephant (*Loxodonta africana*). *Brain Behav. Evol.* **75**, 251–261 (2010).
90. Linsenmeier, R. A. & Zhang, H. F. Retinal oxygen: from animals to humans. *Prog. Retin. Eye Res.* **58**, 115–151 (2017).
91. Vaiman, M., Abuita, R. & Bekerman, I. Optic nerve sheath diameters in healthy adults measured by computer tomography. *Int. J. Ophthalmol.* **8**, 1240–1244 (2015).
92. Robles, E., Laurell, E. & Baier, H. The retinal projectome reveals brain-area-specific visual representations generated by ganglion cell diversity. *Curr. Biol.* **24**, 2085–2096 (2014).  
**Study on larval zebrafish showing that RGCs with similar dendritic stratification profiles can exhibit very distinct central wiring motifs.**
93. Antinucci, P., Suleyman, O., Monfries, C. & Hindges, R. Neural mechanisms generating orientation selectivity in the retina. *Curr. Biol.* **26**, 1802–1815 (2016).  
**Study on larval zebrafish showing that orientation-selective computations begin at the level of bipolar cell interactions with specific amacrine cells.**
94. Johnston, J. et al. A retinal circuit generating a dynamic predictive code for oriented features. *Neuron* **102**, 1211–1222 (2019).  
**Study on larval zebrafish extending the results from Antinucci et al. (2016) to show how distinct orientation-selective inputs from bipolar cells lead to the possibility to build highly complex response properties at the level of RGCs.**
95. Hildebrand, D. G. C. et al. Whole-brain serial-section electron microscopy in larval zebrafish. *Nature* **545**, 345–349 (2017).
96. Faisal, A. A., White, J. A. & Laughlin, S. B. Ion-channel noise places limits on the miniaturization of the brain's wiring. *Curr. Biol.* **15**, 1143–1149 (2005).
97. Faisal, A. A. & Laughlin, S. B. Stochastic simulations on the reliability of action potential propagation in thin axons. *PLOS Comput. Biol.* **3**, e79 (2007).
98. Baden, T. & Osorio, D. The retinal basis of vertebrate color vision. *Annu. Rev. Vis. Sci.* **5**, 177–200 (2019).
99. Kelber, A. & Osorio, D. From spectral information to animal colour vision: experiments and concepts. *Proc. R. Soc. B Biol. Sci.* **277**, 1617–1625 (2010).
100. Theiss, S. M., Davies, W. I. L., Collin, S. P., Hunt, D. M. & Hart, N. S. Cone monochromacy and visual pigment spectral tuning in wobbegong sharks. *Biol. Lett.* **8**, 1019–1022 (2012).
101. Peichl, L. Diversity of mammalian photoreceptor properties: adaptations to habitat and lifestyle? *Anat. Rec. A Discov. Mol. Cell. Evol. Biol.* **287**, 1001–1012 (2005).
102. Rocha, F. A. F., Saito, C. A., Silveira, L. C. L., De Souza, J. M. & Ventura, D. F. Twelve chromatically opponent ganglion cell types in turtle retina. *Vis. Neurosci.* **25**, 307–315 (2008).
103. Marshak, D. W. & Mills, S. L. Short-wavelength cone-opponent retinal ganglion cells in mammals. *Vis. Neurosci.* **31**, 165–175 (2014).
104. Kalinina, A. V. Quantity and topography of frog's retinal ganglion cells. *Vis. Res.* **16**, 929–934 (1976).
105. Buchsbaum, G. & Gottschalk, A. Trichromacy, opponent colours coding and optimum colour information transmission in the retina. *Proc. R. Soc. Lond. B Biol. Sci.* **220**, 89–113 (1983).
106. Lewis, A. & Zhao, L. Are cone sensitivities determined by natural color statistics? *J. Vis.* **6**, 285–302 (2006).
107. Osorio, D. & Vorobyev, M. A review of the evolution of animal colour vision and visual communication signals. *Vis. Res.* **48**, 2042–2051 (2008).
108. Hughes, A. Topographical relationships between the anatomy and physiology of the rabbit visual system. *Doc. Ophthalmol.* **30**, 33–159 (1971).
109. Sherman, S. M. Visual fields of cats with cortical and tectal lesions. *Science* **185**, 355–357 (1974).
110. Meyer, A. F., Poort, J., O'Keefe, J., Sahani, M. & Linden, J. F. A head-mounted camera system integrates detailed behavioral monitoring with multichannel electrophysiology in freely moving mice. *Neuron* **100**, 46–60 (2018).
111. Wallace, D. J. et al. Rats maintain an overhead binocular field at the expense of constant fusion. *Nature* **498**, 65–69 (2013).
112. Mitkus, M., Olsson, P., Toomey, M. B., Corbo, J. C. & Kelber, A. Specialized photoreceptor composition in the raptor fovea. *J. Comp. Neurol.* **529**, 2152–2163 (2017).  
**Study showing that the central but not the temporal foveas of raptors tend to lack the double cones that are traditionally associated with achromatic high-spatial-acuity vision. These birds might therefore use high-resolution tetrachromatic vision for high-spatial-acuity tasks.**
113. Pettigrew, J. D., Collin, S. P. & Ott, M. Convergence of specialised behaviour, eye movements and visual optics in the sandlance (Teleostei) and the chameleon (Reptilia). *Curr. Biol.* **9**, 421–424 (1999).
114. Rucci, M. & Poletti, M. Control and functions of fixational eye movements. *Annu. Rev. Vis. Sci.* **1**, 499–518 (2015).
115. Samonds, J. M., Geisler, W. S. & Priebe, N. J. Natural image and receptive field statistics predict saccade sizes. *Nat. Neurosci.* **21**, 1591–1599 (2018).
116. Manookin, M. B., Patterson, S. S. & Linehan, C. M. Neural mechanisms mediating motion sensitivity in parasol ganglion cells of the primate retina. *Neuron* **97**, 1327–1340 (2018).
117. Yilmaz, M. & Meister, M. rapid innate defensive responses of mice to looming visual stimuli. *Curr. Biol.* **23**, 2011–2015 (2013).
118. Janssen, J. Searching for zooplankton just outside Snell's window. *Limmol. Oceanogr.* **26**, 1168–1171 (1981).
119. Peichl, L. Die Augen der Säugetiere: unterschiedliche Blicke in die Welt. *Biol. Unserer Zeit* **27**, 96–105 (1997).
120. Hughes, A. A comparison of retinal ganglion cell topography in the plains and tree kangaroo. *J. Physiol.* **244**, 61P–63P (1975).
121. Sablin, M. V. & Khlopachev, G. A. The earliest ice age dogs: evidence from Eliseevichi 1. *Curr. Anthropol.* **43**, 795–799 (2002).
122. Peichl, L. Topography of ganglion-cells in the dog and wolf retina. *J. Comp. Neurol.* **324**, 603–620 (1992).
123. Coimbra, J. P. & Manger, P. R. Retinal ganglion cell topography and spatial resolving power in the white rhinoceros (*Ceratotherium simum*). *J. Comp. Neurol.* **525**, 2484–2498 (2017).
124. Coimbra, J. P., Bertelsen, M. F. & Manger, P. R. Retinal ganglion cell topography and spatial resolving power in the river hippopotamus (*Hippopotamus amphibius*). *J. Comp. Neurol.* **525**, 2499–2513 (2017).
125. Collin, S. P. Behavioural ecology and retinal cell topography. in *Adaptive Mechanisms in the Ecology of Vision* (eds Archer, S. N. et al.) 509–535 (Springer, 1999).
126. Coimbra, J. P., Collin, S. P. & Hart, N. S. Topographic specializations in the retinal ganglion cell layer correlate with lateralized visual behavior, ecology, and evolution in cockatoos. *J. Comp. Neurol.* **522**, 3363–3385 (2014).
127. Tucker, V. A. The deep fovea, sideways vision and spiral flight paths in raptors. *J. Exp. Biol.* **203**, 3745–3754 (2000).
128. Kolb, H. & Marshak, D. The midjet pathways of the primate retina. *Doc. Ophthalmol.* **106**, 67–81 (2003).
129. Baudin, J., Angueyra, J. M., Sinha, R. & Rieke, F. S-cone photoreceptors in the primate retina are functionally distinct from L and M cones. *Elife* **8**, e39166 (2019).
130. Harvey, B. M. & Dumoulin, S. O. The relationship between cortical magnification factor and population receptive field size in human visual cortex: constancies in cortical architecture. *J. Neurosci.* **31**, 13604–13612 (2011).
131. Szél, A. et al. Unique topographic separation of two spectral classes of cones in the mouse retina. *J. Comp. Neurol.* **325**, 327–342 (1992).
132. Röhlich, P., van Veen, T. & Szél, A. Two different visual pigments in one retinal cone cell. *Neuron* **13**, 1159–1166 (1994).
133. Haverkamp, S. et al. The primordial, blue-cone color system of the mouse retina. *J. Neurosci.* **25**, 5438–5445 (2005).
134. Tan, Z., Sun, W., Chen, T.-W., Kim, D. & Ji, N. Neuronal representation of ultraviolet visual stimuli in mouse primary visual cortex. *Sci. Rep.* **5**, 12597 (2015).
135. Denman, D. J. et al. Mouse color and wavelength-specific luminance contrast sensitivity are non-uniform across visual space. *Elife* **7**, e31209 (2018).
136. Joesch, M. & Meister, M. A neuronal circuit for colour vision based on rod-cone opponency. *Nature* **532**, 236–239 (2016).
137. Chang, L., Breuninger, T. & Euler, T. Chromatic coding from cone-type unselective circuits in the mouse retina. *Neuron* **77**, 559–571 (2013).
138. Kim, I.-J., Zhang, Y., Yamagata, M., Meister, M. & Sanes, J. R. Molecular identification of a retinal cell type that responds to upward motion. *Nature* **452**, 478–482 (2008).
139. Peichl, L. & Ott, H. & Boycott, B. B. Alpha ganglion cells in mammalian retinae. *Proc. R. Soc. Lond. Ser. B Biol. Sci.* **231**, 169–197 (1987).
140. Barlow, H. B., Hill, R. M. & Levick, W. R. Rabbit retinal ganglion cells responding selectively to direction and speed of image motion in the rabbit. *J. Physiol.* **173**, 377–407 (1964).
141. Krapp, H. G. & Hengstenberg, R. Estimation of self-motion by optic flow processing in single visual interneurons. *Nature* **384**, 463–466 (1996).
142. Yu, W. Q. et al. synaptic convergence patterns onto retinal ganglion cells are preserved despite topographic variation in pre- and postsynaptic territories. *Cell Rep.* **25**, 2017–2026 (2018).
143. Seung, H. S. & Sümbül, U. Neuronal cell types and connectivity: lessons from the retina. *Neuron* **83**, 1262–1272 (2014).
144. Vlasits, A. L., Euler, T. & Franke, K. Function first: classifying cell types and circuits of the retina. *Curr. Opin. Neurobiol.* **56**, 8–15 (2019).
145. Laughlin, S. Matching coding to scenes to enhance efficiency. in *Physical and Biological Processing of Images* (eds Braddick O. J. & Sleight A. C.) 42–52 (Springer, 1983).
146. Atick, J. J. & Redlich, A. N. Towards a theory of early visual processing. *Neural Comput.* **2**, 308–320 (2008).
147. Simoncelli, E. P. & Olshausen, B. A. Natural image statistics and neural representation. *Annu. Rev. Neurosci.* **24**, 1193–1216 (2001).
148. van der Schaaf, A. & van Hateren, J. H. Modelling the power spectra of natural images: statistics and information. *Vis. Res.* **36**, 2759–2770 (1996).
149. Atick, J. J. & Redlich, A. N. What does the retina know about natural scenes? *Neural Comput.* **4**, 196–210 (1992).
150. Doi, E. et al. Efficient coding of spatial information in the primate retina. *J. Neurosci.* **32**, 16256–16264 (2012).
151. Sinz, F. & Bethge, M. Temporal adaptation enhances efficient contrast gain control on Natural Images. *PLOS Comput. Biol.* **9**, e1002889 (2013).
152. Pitkow, X. & Meister, M. Decorrelation and efficient coding by retinal ganglion cells. *Nat. Neurosci.* **15**, 628–635 (2012).
153. Dacey, D. M. Primate retina: cell types, circuits and color opponency. *Prog. Retin. Eye Res.* **18**, 737–763 (1999).
154. Rheau, B. A. et al. Single cell transcriptome profiling of retinal ganglion cells identifies cellular subtypes. *Nat. Commun.* **9**, 2759 (2018).
155. Gjorgjieva, J., Sompolinsky, H. & Meister, M. Benefits of pathway splitting in sensory coding. *J. Neurosci.* **34**, 12127–12144 (2014).
156. Kastner, D. B., Baccus, S. A. & Sharpee, T. O. Critical and maximally informative encoding between neural populations in the retina. *Proc. Natl Acad. Sci. USA* **112**, 2533–2538 (2015).
157. Ocko, S. A., Lindsey, J., Ganguli, S. & Deny, S. The emergence of multiple retinal cell types through efficient coding of natural movies. Preprint at *bioRxiv* <https://doi.org/10.1101/458737> (2018).  
**Theoretical study showing that a small number of RGC types with simple centre-surround receptive fields can be principally explained by the statistics of natural scenes.**
158. Golisch, T. & Meister, M. Review eye smarter than scientists believed: neural computations in circuits of the retina. *Neuron* **65**, 150–164 (2009).
159. Turner, M. H., Sanchez Giraldo, L. G., Schwartz, O. & Rieke, F. Stimulus- and goal-oriented frameworks for understanding natural vision. *Nat. Neurosci.* **22**, 15–24 (2019).
160. Turner, M. H., Schwartz, G. W. & Rieke, F. Receptive field center-surround interactions mediate context-dependent spatial contrast encoding in the retina. *eLife* **7**, e38841 (2018).



161. Schwartz, G. W. et al. The spatial structure of a nonlinear receptive field. *Nat. Neurosci.* **15**, 1572–1580 (2012).
162. Freeman, J. et al. Mapping nonlinear receptive field structure in primate retina at single cone resolution. *eLife* **4**, 284–299 (2015).
163. Liu, J. K. et al. Spike-triggered covariance analysis reveals phenomenological diversity of contrast adaptation in the retina. *PLOS Comput. Biol.* **11**, e1004425 (2015).
164. Real, E., Asari, H., Gollisch, T. & Meister, M. Neural circuit inference from function to structure. *Curr. Biol.* **27**, 189–198 (2017).
165. McIntosh, L. T., Maheswaranathan, N., Nayeibi, A., Ganguli, S. & Baccus, S. A. Deep learning models of the retinal response to natural scenes. *Adv. Neural. Inf. Process. Syst.* **29**, 1369–1377 (2016).
166. Maheswaranathan, N., Kastner, D. B., Baccus, S. A. & Ganguli, S. Inferring hidden structure in multilayered neural circuits. *PLOS Comput. Biol.* **14**, e1006291 (2018).
167. Tkačik, G. et al. Natural images from the birthplace of the human eye. *PLOS ONE* **6**, e20409 (2011).
168. Tedore, C. & Nilsson, D. E. Avian UV vision enhances leaf surface contrasts in forest environments. *Nat. Commun.* **10**, 238 (2019).
169. Nevala, N. E. & Baden, T. A low-cost hyperspectral scanner for natural imaging and the study of animal colour vision above and under water. *Sci. Rep.* **9**, 10799 (2019).
170. Zeil, J., Boeddeker, N. & Hemmi, J. M. Vision and the organization of behaviour. *Curr. Biol.* **18**, R320–R323 (2008).
171. Lamb, T. D., Collin, S. P., Pugh, E. N. Jr. Evolution of the vertebrate eye: opsins, photoreceptors, retina and eye cup. *Nat. Rev. Neurosci.* **8**, 960–976 (2007). **Key account of the vertebrate eye's evolutionary history.**
172. Young, G. C. Early evolution of the vertebrate eye — fossil evidence. *Evol. Educ. Outreach* **1**, 427–438 (2008).
173. Fritzsche, B. & Collin, S. P. Dendritic distribution of two populations of ganglion cells and the retinopetal fibers in the retina of the silver lamprey (*Ichthyomyzon unicuspis*). *Vis. Neurosci.* **4**, 535–545 (1990).
174. Morris, S. C. & Caron, J.-B. A primitive fish from the Cambrian of North America. *Nature* **512**, 419–422 (2014).
175. Xian-Guang, H., Aldridge, R. J., Siveter, D. J., Siveter, D. J. & Xiang-Hong, F. New evidence on the anatomy and phylogeny of the earliest vertebrates. *Proc. R. Soc. B Biol. Sci.* **269**, 1865–1869 (2002).
176. Shu, D. G. et al. Lower Cambrian vertebrates from south China. *Nature* **402**, 42–46 (1999).
177. Fletcher, L. N. et al. Classification of retinal ganglion cells in the southern hemisphere lamprey *Geotria australis* (Cyclostomata). *J. Comp. Neurol.* **522**, 750–771 (2014).
178. Collin, S. P., Davies, W. L., Hart, N. S. & Hunt, D. M. The evolution of early vertebrate photoreceptors. *Phil. Trans. R. Soc. B Biol. Sci.* **364**, 2925–2940 (2009).
179. Sallan, L., Friedman, M., Sansom, R. S., Bird, C. M. & Sansom, I. J. The nearshore cradle of early vertebrate diversification. *Science* **362**, 460–464 (2018).
180. Brazeau, M. D. & Friedman, M. The origin and early phylogenetic history of jawed vertebrates. *Nature* **520**, 490–497 (2015).
181. Country, M. W. Retinal metabolism: a comparative look at energetics in the retina. *Brain Res.* **1672**, 50–57 (2017).
182. Wright, A. F., Chakarova, C. F., Abd El-Aziz, M. M. & Bhattacharya, S. S. Photoreceptor degeneration: genetic and mechanistic dissection of a complex trait. *Nat. Rev. Genet.* **11**, 273–284 (2010).
183. Krishnan, J. & Rohner, N. Cavefish and the basis for eye loss. *Phil. Trans. R. Soc. B Biol. Sci.* **372**, 20150487 (2017).
184. Gore, A. V. et al. An epigenetic mechanism for cavefish eye degeneration. *Nat. Ecol. Evol.* **2**, 1155–1160 (2018).
185. Merriman, D. K., Sajdak, B. S., Li, W. & Jones, B. W. Seasonal and post-trauma remodeling in cone-dominant ground squirrel retina. *Exp. Eye Res.* **150**, 90–105 (2016).
186. Emran, F., Rihel, J., Adolph, A. R. & Dowling, J. E. Zebrafish larvae lose vision at night. *Proc. Natl Acad. Sci. USA* **107**, 6034–6039 (2010).
187. Adolph, A. R. Temporal tuning and nonlinearity of intraretinal pathways in turtle: effects of temperature, stimulus intensity, and size. *Biol. Cybern.* **52**, 59–69 (1985).
188. Ankel-Simons, F. & Rasmussen, D. T. Diurnality, nocturnality, and the evolution of primate visual systems. *Am. J. Phys. Anthropol.* **47**, 100–117 (2008).
189. Cronin, T. W. & Bok, M. J. Photoreception and vision in the ultraviolet. *J. Exp. Biol.* **219**, 2790–2801 (2016).
190. Muaddi, J. A. & Jamal, M. A. Solar spectrum at depth in water. *Renew. Energy* **1**, 31–35 (1991).
191. Williams, R. W., Strom, R. C. & Goldowitz, D. Natural variation in neuron number in mice is linked to a major quantitative trait locus on Chr 11. *J. Neurosci.* **18**, 138–146 (2018).
192. Kolb H. in *Webvision: The Organization of the Retina and Visual System* (eds Kolb, H. et al.) (Univ. Utah Health Sciences Center, 1995).
193. McMains, E., Krishnan, V., Prasad, S. & Gleason, E. Expression and localization of CLC chloride transport proteins in the avian retina. *PLOS ONE* **6**, e17647 (2011).
194. Gramage, E., Li, J. & Hitchcock, P. The expression and function of midline in the vertebrate retina. *Br. J. Pharmacol.* **171**, 913–923 (2014).
195. Almeida, A. D. et al. Spectrum of fates: a new approach to the study of the developing zebrafish retina. *Development* **141**, 1971–1980 (2014).
196. Deng, P. et al. Localization of neurotransmitters and calcium binding proteins to neurons of salamander and mudpuppy retinas. *Vis. Res.* **41**, 1771–1783 (2001).
197. Holmberg, K. Fine structure of the optic tract in the Atlantic hagfish, *Myxine glutinosa*. *Acta Zool.* **53**, 165–171 (1972).
198. Pita, D., Moore, B. A., Tyrrell, L. P. & Fernández-Juricic, E. Vision in two cyprinid fish: implications for collective behavior. *PeerJ* **3**, e1113 (2015).
199. Dalton, B. E., de Bussorilles, F., Marshall, N. J. & Carleton, K. L. Retinal specialization through spatially varying cell densities and opsin coexpression in cichlid fish. *J. Exp. Biol.* **220**, 266–277 (2017).
200. Wagner, H. J., Fröhlich, E., Negishi, K. & Collin, S. P. The eyes of deep-sea fish II. Functional morphology of the retina. *Prog. Retin. Eye Res.* **17**, 637–685 (1998).
201. Hitchcock, P. & Easter, S. Retinal ganglion cells in goldfish: a qualitative classification into four morphological types, and a quantitative study of the development of one of them. *J. Neurosci.* **6**, 1037–1050 (1986).
202. Dunlop, S. A. & Beazley, L. D. Changing retinal ganglion cell distribution in the frog *Heleoporus eyrei*. *J. Comp. Neurol.* **202**, 221–236 (1981).
203. Nguyen, V. S. & Straznicki, C. The development and the topographic organization of the retinal ganglion cell layer in *Bufo marinus*. *Exp. Brain Res.* **75**, 345–353 (1989).
204. Graydon, M. L. & Giorgi, P. P. Topography of the retinal ganglion cell layer of *Xenopus*. *J. Anat.* **139**, 145–157 (1984).
205. Zhang, J., Yang, Z. & Wu, S. M. Immunocytochemical analysis of spatial organization of photoreceptors and amacrine and ganglion cells in the tiger salamander retina. *Vis. Neurosci.* **21**, 157–166 (2004).
206. Pushchin, I. I. & Karetin, Y. A. Retinal ganglion cells in the eastern newt *Notophthalmus viridescens*: Topography, morphology, and diversity. *J. Comp. Neurol.* **516**, 533–552 (2009).
207. Hauzman, E., Bonci, D. M. O. & Ventura, D. F. in *Retinal Topographic Maps: A Glimpse into the Animals' Visual World, Sensory Nervous System* (ed. Heinbockel T.) (IntechOpen, 2018).
208. Nagloo, N., Collin, S. P., Hemmi, J. M. & Hart, N. S. Spatial resolving power and spectral sensitivity of the saltwater crocodile, *Crocodylus porosus*, and the freshwater crocodile, *Crocodylus johnstoni*. *J. Exp. Biol.* **219**, 1394–1404 (2016).
209. Hassni, M. El, M'hamed, S. B., Réperant, J. & Bennis, M. Quantitative and topographical study of retinal ganglion cells in the chameleon (*Chamaeleo chamaeleon*). *Brain Res. Bull.* **44**, 621–625 (1997).
210. Bennis, M. et al. A quantitative ultrastructural study of the optic nerve of the chameleon. *Brain Behav. Evol.* **58**, 49–60 (2001).
211. New, S. T. D. & Bull, C. M. Retinal ganglion cell topography and visual acuity of the sleepy lizard (*Tiliqua rugosa*). *J. Comp. Physiol. A Neuroethol. Sens. Neural Behav. Physiol.* **197**, 703–709 (2011).
212. Hayes, B. P. & Brooke, M. D. L. Retinal ganglion cell distribution and behaviour in procellariiform seabirds. *Vis. Res.* **30**, 1277–1289 (1990).
213. Boire, D., Dufour, J. S., Théoret, H. & Ptito, M. Quantitative analysis of the retinal ganglion cell layer in the ostrich, *Struthio camelus*. *Brain Behav. Evol.* **58**, 343–355 (2001).
214. Suburo, A. M., Herrero, M. V. & Scolaro, J. A. Regionalization of the ganglion cell layer in the retina of the Magellanic penguin (*Spheniscus magellanicus*). *Colon. Waterbirds* **14**, 17 (1991).
215. Coimbra, J. P., Nolan, P. M., Collin, S. P. & Hart, N. S. Retinal ganglion cell topography and spatial resolving power in penguins. *Brain Behav. Evol.* **80**, 254–268 (2012).
216. Wathey, J. C. & Pettigrew, J. D. Quantitative analysis of the retinal ganglion cell layer and optic nerve of the barn owl *Tyto alba*. *Brain Behav. Evol.* **33**, 279–292 (1989).
217. Lisney, T. J., Iwaniuk, A. N., Bandet, M. V. & Wylie, D. R. Eye shape and retinal topography in owls (Aves: Strigiformes). *Brain Behav. Evol.* **79**, 218–236 (2012).
218. Bravo, H. & Pettigrew, J. D. The distribution of neurons projecting from the retina and visual cortex to the thalamus and tectum opticum of the barn owl, *Tyto alba*, and the burrowing owl, *Speotyto cunicularia*. *J. Comp. Neurol.* **199**, 419–441 (1981).
219. Lisney, T. J. et al. Interspecific variation in eye shape and retinal topography in seven species of galliform bird (Aves: Galliformes: Phasianidae). *J. Comp. Physiol. A Neuroethol. Sens. Neural Behav. Physiol.* **198**, 717–731 (2012).
220. Lisney, T. J. et al. Ecomorphology of eye shape and retinal topography in waterfowl (Aves: Anseriformes: Anatidae) with different foraging modes. *J. Comp. Physiol. A Neuroethol. Sens. Neural Behav. Physiol.* **199**, 385–402 (2013).
221. Hart, N. S. Vision in the peafowl (Aves: Pavo cristatus). *J. Exp. Biol.* **205**, 3925–3935 (2002).
222. Moore, B. A., Pita, D., Tyrrell, L. P. & Fernandez-Juricic, E. Vision in avian emberizid foragers: maximizing both binocular vision and fronto-lateral visual acuity. *J. Exp. Biol.* **218**, 1347–1358 (2015).
223. Moore, B. A., Doppler, M., Young, J. E. & Fernández-Juricic, E. Interspecific differences in the visual system and scanning behavior of three forest passerines that form heterospecific flocks. *J. Comp. Physiol. A Neuroethol. Sens. Neural Behav. Physiol.* **199**, 263–277 (2013).
224. Coimbra, J. P., Collin, S. P. & Hart, N. S. Topographic specializations in the retinal ganglion cell layer of Australian passerines. *J. Comp. Neurol.* **522**, 3609–3628 (2014).
225. Hayes, B. P. & Holden, A. L. The distribution of displaced ganglion cells in the retina of the pigeon. *Exp. Brain Res.* **49**, 181–188 (1983).
226. Coimbra, J. P., Videira Marceliano, M. L., Da Silveira Andrade-Da-Costa, B. L. & Yamada, E. S. The retina of tyrant flycatchers: Topographic organization of neuronal density and size in the ganglion cell layer of the great kiskadee *Pitangus sulphuratus* and the rusty margined flycatcher *Myiozetetes cayanensis* (Aves: Tyrannidae). *Brain Behav. Evol.* **68**, 15–25 (2006).
227. Coimbra, J. P. et al. Number and distribution of neurons in the retinal ganglion cell layer in relation to foraging behaviors of tyrant flycatchers. *J. Comp. Neurol.* **514**, 66–73 (2009).
228. Krabichler, Q., Vega-Zuniga, T., Morales, C., Luksch, H. & Marin, G. J. The visual system of a palaeognathous bird: visual field, retinal topography and retino-central connections in the Chilean tinamou (*Nothoprocta perdicaria*). *J. Comp. Neurol.* **523**, 226–250 (2015).
229. Moroney, M. K. & Pettigrew, J. D. Some observations on the visual optics of kingfishers (Aves, Coraciiformes, Alcedinidae). *J. Comp. Physiol. A* **160**, 137–149 (1987).
230. Do-Nascimento, J. L., Do-Nascimento, R. S., Damasceno, B. A. & Silveira, L. C. The neurons of the retinal ganglion cell layer of the guinea pig: quantitative analysis of their distribution and size. *Braz. J. Med. Biol. Res.* **24**, 199–214 (1991).
231. Coimbra, J. P., Hart, N. S., Collin, S. P. & Manger, P. R. Scene from above: retinal ganglion cell topography and spatial resolving power in the giraffe (*Giraffa camelopardalis*). *J. Comp. Neurol.* **521**, 2042–2057 (2013).
232. Mass, A. M. Visual field organization and retinal resolution in the beluga whale *Delphinapterus leucas* (Pallas). *Dokl. Biol. Sci.* **381**, 555–558 (2001).
233. Schall, J. D., Perry, V. H. & Leventhal, A. G. Ganglion cell dendritic structure and retinal topography in the rat. *J. Comp. Neurol.* **257**, 160–165 (1987).



234. Curcio, C. A. & Allen, K. A. Topography of ganglion cells in human retina. *J. Comp. Neurol.* **300**, 5–25 (1990).
235. Stabio, M. E. et al. A novel map of the mouse eye for orienting retinal topography in anatomical space. *J. Comp. Neurol.* **526**, 1749–1759 (2018).
236. Szél, A. & Roehlich, P. Two cone types of rat retina detected by anti-visual pigment antibodies. *Exp. Eye Res.* **55**, 47–52 (1992).
237. Liu, J. K. et al. Inference of neuronal functional circuitry with spike-triggered non-negative matrix factorization. *Nat. Commun.* **8**, 149 (2017).

## Acknowledgements

The authors thank L. Peichl, J. Coimbra, T. Lisney and S. Collin for very helpful discussions as well as the four anonymous

reviewers for their insightful comments. T.B. also acknowledges support from the FENS-Kavli Network of Excellence and from the EMBO Young Investigator Programme. Funding was provided by the European Research Council (Starting Grant NeuroVisEco 677687, T.B.), UK Research and Innovation (Biotechnology and Biological Sciences Research Council, BB/R014817/1, and Medical Research Council, MC\_PC\_15071, T.B.), the Leverhulme Trust (PLP-2017-005, T.B.), the Lister Institute for Preventive Medicine (T.B.), the German Research Foundation (SFB 1233 — project number 276693517, T.E. and P.B.; SPP 2041: EU42/9-1, T.E.; BE5601/2, P.B.; BE5601/4, P.B.), the National Eye Institute (1R01EY023766-01A1, T.E.), and the German Ministry for Education and Research (FKZ 01GQ1601, P.B.).

## Author contributions

The authors contributed equally to all aspects of the article.

## Competing interests

The authors declare no competing interests.

## Peer review information

*Nature Reviews Neuroscience* thanks G. Field, G. Schwartz and the other, anonymous, reviewer(s) for their contribution to the peer review of this work.

## Publisher's note

Springer Nature remains neutral with regard to jurisdictional claims in published maps and institutional affiliations.

## Supplementary information

Supplementary information is available for this paper at <https://doi.org/10.1038/s41585-019-0242-1>.

© Springer Nature Limited 2019